Eur. Phys. J. C 36, 483–501 (2004)
Digital Object Identifier (DOI) 10.1140/epjc/s2004-01959-1

THE EUROPEAN PHYSICAL JOURNAL C

Spectra and decays of $\pi\pi$ and πK atoms

J. Schweizer[a]

Institute for Theoretical Physics, University of Bern, Sidlerstr. 5, 3012 Bern, Switzerland

Received: 9 May 2004 /
Published online: 23 July 2004 –

Abstract. We describe the spectra and decays of $\pi^+\pi^-$ and $\pi^\pm K^\mp$ atoms within a non-relativistic effective field theory. The evaluations of the energy shifts and widths are performed at next-to-leading order in isospin symmetry breaking. We provide general formulae for all S-states, and discuss the states with angular momentum one in some detail. The prediction for the lifetime of the $\pi^\pm K^\mp$ atom in its ground state yields $\tau_{10} = (3.7 \pm 0.4) \cdot 10^{-15}$ s.

1 Introduction

The DIRAC collaboration [1] at CERN has measured the lifetime of pionium in its ground state, and the preliminary result yields $\tau_{\pi,10} = [3.1^{+0.9}_{-0.7}(\text{stat}) \pm 1(\text{syst})] \cdot 10^{-15}$ s [2]. A lifetime measurement of pionium at the 10% level allows one to determine the S-wave $\pi\pi$ scattering length difference $|a_0^0 - a_0^2|$ at 5% accuracy. The measurement can then be compared with theoretical predictions for the S-wave scattering lengths [3–5] and with the results coming from scattering experiments [6]. Particularly exciting is the fact that this enterprise subjects chiral perturbation theory to a very sensitive test [7]. New measurements are proposed for CERN PS, J-PARC and GSI [8]. These experiments aim to measure the lifetime of $\pi^+\pi^-$ and $\pi^\pm K^\mp$ atoms simultaneously.

In order to extract the scattering lengths from such future precision measurements, the theoretical expressions for the energy shifts and decay widths of the $\pi^+\pi^-$ and $\pi^\pm K^\mp$ atoms must be known to a precision that matches the experimental accuracy. Nearly fifty years ago, Deser et al. [9] derived the leading order formulae for the decay width and the energy shift in pionic hydrogen. Similar relations exist for $\pi^+\pi^-$ and $\pi^\pm K^\mp$ atoms [10,11], which decay due to the strong interactions into $2\pi^0$ and $\pi^0 K^0$, respectively. Theoretical investigations on the spectrum and the decay of pionium have been performed beyond leading order in several settings. Potential scattering has been used [12–14] as well as field-theoretical methods [15–20]. In particular, the lifetime of pionium was studied by the use of the Bethe–Salpeter equation [19] and in the framework of the quasipotential-constraint theory approach [20]. The width of the $\pi^+\pi^-$ atom has also been analyzed within a non-relativistic effective field theory [21–23], which was originally developed for bound states in QED by Caswell and Lepage [24]. The non-relativistic framework has proven to be a very efficient method to evaluate bound-state characteristics. It was further applied to the ground state of pionic hydrogen [25–27] and very recently to the energy levels and decay widths of kaonic hydrogen [28]. Within the non-relativistic effective field theory the isospin symmetry breaking corrections to the Deser-type formulae can be evaluated systematically. In [21–23,29,30] the lifetime of pionium was evaluated at next-to-leading order in the isospin breaking parameters $\alpha \simeq 1/137$ and $(m_u - m_d)^2$.

We presented in [31], the results for the S-wave decay widths and strong energy shifts of $\pi^+\pi^-$ and $\pi^\pm K^\mp$ atoms at next-to-leading order in isospin symmetry breaking. Further, for the lifetime as well as for the first two energy-level shifts, a numerical analysis was carried out. The aim of this article is to provide the details that have been omitted in [31]. Chiral perturbation theory (ChPT) allows one to relate the result for the width of the $\pi^\pm K^\mp$ atom to the isospin odd πK scattering lengths a_0^-, while the strong energy shift is proportional to the sum of isospin even and odd scattering lengths $a_0^+ + a_0^-$. The values for a_0^+ and a_0^-, used in the numerical evaluation of the widths and strong energy shifts, stem from the recent analysis of πK scattering from Roy- and Steiner-type equations [33]. Within ChPT, the πK scattering lengths have been worked out at one-loop accuracy [34–36], and very recently even the chiral expansion of the πK scattering amplitude at next-to-next-to-leading order became available [37]. Particularly interesting is that the isospin even scattering lengths a_0^+ depends on the low-energy constant L_6^{r} [38], and this coupling is related to the flavor dependence of the quark condensate [39].

This paper is organized as follows: The general features of $\pi^+\pi^-$ and $\pi^\pm K^\mp$ atoms are described in Sect. 2. The non-relativistic effective field-theory approach is illustrated in Sect. 3 by means of the $\pi^- K^+$ atom. The discussion includes the Hamiltonian, the master equation, and the matching to the relativistic πK amplitudes. In Sect. 4, we present the results for the decay widths and

[a] e-mail: schweizer@itp.unibe.ch

strong energy shifts of the $\pi^\pm K^\mp$ and $\pi^+\pi^-$ atoms at next-to-leading order in isospin symmetry breaking. The role of transverse photons is discussed in Sect. 5. Transverse photons do contribute to the electromagnetic part of the energy shift. The pure QED contributions have been worked out a long time ago, based on the Bethe–Salpeter equation [40], the quasipotential approach [41,42] and an improved Coulomb potential [43]. We reproduced this result within the non-relativistic framework. We further estimate the contributions from transverse photons to the decay width of the π^-K^+ atom and show that they vanish at next-to-leading order in isospin symmetry breaking. The contributions generated by the vacuum polarization of the electron [22,25,44] are discussed in Sect. 6. Formally of higher order in α, they are numerically not negligible. A numerical analysis of the widths and the energy-level shifts is carried out in Sect. 7 at $\mathcal{O}(p^4, e^2p^2)$ in the chiral expansion.

2 General features of $\pi\pi$ and πK atoms

In this section, we describe the general features of the systems that we are going to study. The $\pi^+\pi^-$ and $\pi^\pm K^\mp$ atoms are highly non-relativistic, loosely bound systems, mainly formed by the Coulomb interaction. The average momentum of the constituents in the CM frame lies in the MeV range. Further, their decay widths $\sim 0.2\,\text{eV}$ are much smaller than the binding energies $\sim 10^3\,\text{eV}$ involved. The $\pi^+\pi^-$ atom in its ground-state decays predominantly into a pair of two neutral pions, through the strong transition $\pi^+\pi^- \to \pi^0\pi^0$. The decay width into two photons is suppressed by the factor $4\cdot 10^{-3}$ [1,29]. For a detailed discussion of the decay channels of pionium, we refer to [23]. The decays of the π^-K^+ atom have to conserve strangeness. Apart from the dominant S-wave decay channel into π^0K^0, the only allowed decays are therefore $K^0 + n_1\gamma + n_2e^+e^-$ and $\pi^0K^0 + n_1\gamma + n_2e^+e^-$, where $n_1 + n_2 > 0$. Here n_1 and n_2 denotes the number of photons and e^+e^- pairs, respectively. In the relativistic theory, the odd intrinsic parity process $\pi^-K^+ \to K^0 + 2\gamma$ corresponds to a local interaction in the Wess–Zumino–Witten term [45], while the transition $\pi^-K^+ \to K^0 + \gamma$ occurs not until $\mathcal{O}(p^6)$ [46].

The non-relativistic framework [21,23–25] we are going to apply, provides a systematic expansion in the isospin breaking parameter δ. In the case of pionium, we count α as well as $(m_u - m_d)^2$ as small quantities of order δ. As for the $\pi^\pm K^\mp$ atom, both α and $m_u - m_d$ count as order δ. The different power counting schemes are due to the fact that in QCD, the chiral expansion of the pion mass squared difference $\Delta_\pi = M_{\pi^+}^2 - M_{\pi^0}^2$ is of second order in $m_u - m_d$, while $\Delta_K = M_{K^+}^2 - M_{K^0}^2$ is linear in $m_u - m_d$. At leading and next-to-leading order in isospin symmetry breaking, the $\pi^+\pi^-$ (π^-K^+) atom decays into $\pi^0\pi^0$ (π^0K^0) exclusively. The leading order term for the width is of $\mathcal{O}(\delta^{7/2})$, isospin breaking corrections contribute at order $\delta^{9/2}$. The results for the S-wave decay widths at order $\delta^{9/2}$ are presented in Sects. 4.1 and 4.3. At order δ^5, also other decay channels contribute. In Sect. 5.2, we estimate the order of the various decays.

The energy-level splittings of the $\pi^+\pi^-$ and $\pi^\pm K^\mp$ atoms are induced by both electromagnetic and strong interactions. At order δ^3, the energy shift contributions are exclusively due to strong interactions, while at order δ^4, both electromagnetic and strong interactions contribute. It is both conventional and convenient to split the energy shifts into a strong and an electromagnetic part, according to[1]

$$\Delta E_{nl} = \Delta E_{nl}^{\text{h}} + \Delta E_{nl}^{\text{em}}. \tag{2.1}$$

The expressions for the strong energy shift ΔE_{nl}^{h} at next-to-leading order in isospin symmetry breaking are presented in Sects. 4.2 and 4.3. The electromagnetic part $\Delta E_{nl}^{\text{em}}$ is discussed in Sect. 5.1. Another important correction is generated by the vacuum polarization of the electron. Formally, the vacuum polarization contributes to the energy shift at order δ^5 and to the width at order $\delta^{11/2}$, but these corrections are amplified by powers of the ratio μ_+/m_e. Here μ_+ denotes the reduced mass of the bound system and m_e the electron mass. The vacuum polarization contributions are discussed in Sect. 6.

In what follows, we proceed systematically and discuss in detail the decays and bound-state spectra within the non-relativistic framework.

3 Non-relativistic framework

3.1 Hamiltonian

The Hamiltonian consists of an infinite series of operators with increasing mass dimensions – all operators allowed by gauge invariance, space rotation, parity and time reversal must be included. However, in the evaluation of the decay width and the strong energy shift at next-to-leading order in isospin symmetry breaking, only a few low dimensional operators do actually contribute. For the π^-K^+ atom, the following Hamiltonian achieves the goal:

$$\begin{aligned}\mathbf{H} &= \mathbf{H}_0 + \mathbf{H}_{\text{C}} + \mathbf{H}_{\text{D}} + \mathbf{H}_{\text{S}},\\ \mathbf{H}_\Gamma &= \int \mathrm{d}^3\mathbf{x}\,\mathcal{H}_\Gamma(0,\mathbf{x}), \quad \Gamma = 0, \text{C}, \text{D}, \text{S},\end{aligned} \tag{3.1}$$

with

$$\begin{aligned}\mathcal{H}_0 &= \sum_{i=\pm,0}\left\{\pi_i^\dagger\left(M_{\pi^i} - \frac{\Delta}{2M_{\pi^i}}\right)\pi_i \right.\\ &\qquad \left. + K_i^\dagger\left(M_{K^i} - \frac{\Delta}{2M_{K^i}}\right)K_i\right\},\\ \mathcal{H}_{\text{D}} &= -\sum_{i=\pm,0}\left\{\pi_i^\dagger\left(\frac{\Delta^2}{8M_{\pi^i}^3} + \cdots\right)\pi_i \right.\\ &\qquad \left. + K_i^\dagger\left(\frac{\Delta^2}{8M_{K^i}^3} + \cdots\right)K_i\right\},\end{aligned}$$

[1] Note that this splitting cannot be understood literally, i.e. there are contributions from strong interactions to $\Delta E_{n0}^{\text{em}}$.

$$\mathcal{H}_{\rm C} = -2\pi\alpha \left(\sum_{\pm} \pm\pi_{\pm}^{\dagger}\pi_{\pm} \pm K_{\pm}^{\dagger}K_{\pm} \right) \times \Delta^{-1} \left(\sum_{\pm} \pm\pi_{\pm}^{\dagger}\pi_{\pm} \pm K_{\pm}^{\dagger}K_{\pm} \right),$$

$$\begin{aligned}\mathcal{H}_{\rm S} = & - C_1\pi_-^{\dagger}K_+^{\dagger}\pi_-K_+ - C_2\left(\pi_-^{\dagger}K_+^{\dagger}\pi_0K_0 + \text{h.c.}\right) \\ & - C_3\pi_0^{\dagger}K_0^{\dagger}\pi_0K_0 - C_4\left(\pi_-^{\dagger}\overleftrightarrow{\Delta}K_+^{\dagger}\pi_0K_0 + \text{h.c.}\right) \\ & - C_5\left(\pi_-^{\dagger}\overleftrightarrow{\Delta}K_+^{\dagger}\pi_-K_+ + \text{h.c.}\right) - C_6(\pi_-^{\dagger}\pi_-)\Delta(K_+^{\dagger}K_+) \\ & - C_7\left(\nabla\pi_-^{\dagger}K_+^{\dagger}\nabla\pi_0K_0 + \text{h.c.}\right) + \cdots, \end{aligned} \tag{3.2}$$

where $u\overleftrightarrow{\Delta}v \doteq u\Delta v + v\Delta u$. We work in the CM system and thus omit terms proportional to the CM momentum. The basis of operators with two space derivatives is chosen such that none of them contributes to the S-wave decay width and energy shift at the accuracy we are considering. For this reason, we transformed the operator with two space derivatives on the neutral fields by the use of the equations of motion,

$$\begin{aligned}\pi_-^{\dagger}K_+^{\dagger}\pi_0\overleftrightarrow{\Delta}K_0 = & -4\mu_0(\Sigma_+ - \Sigma_0)\pi_-^{\dagger}K_+^{\dagger}\pi_0K_0 \\ & + \frac{\mu_0}{\mu_+}\pi_-^{\dagger}\overleftrightarrow{\Delta}K_+^{\dagger}\pi_0K_0. \end{aligned} \tag{3.3}$$

For the moment, we further neglect transverse photon contributions. To the accuracy we are working, they do not contribute to the decay width and to the strong energy-level shifts. However, transverse photons do contribute when we work out the electromagnetic energy-level shifts in Sect. 5.1. The non-relativistic Lagrangian in the presence of transverse photons is given in Appendix A. The Hamiltonian in (3.1) is built from the non-relativistic pion and kaon fields

$$\begin{aligned}\pi_i(0,\mathbf{x}) &= \int \mathrm{d}\nu(\mathbf{p})\mathrm{e}^{\mathrm{i}\mathbf{p}\mathbf{x}}\mathbf{a}_i(\mathbf{p}), \\ K_i(0,\mathbf{x}) &= \int \mathrm{d}\nu(\mathbf{p})\mathrm{e}^{\mathrm{i}\mathbf{p}\mathbf{x}}\mathbf{b}_i(\mathbf{p}), \quad i = \pm, 0, \end{aligned} \tag{3.4}$$

with $\mathrm{d}\nu(\mathbf{p}) \doteq \mathrm{d}^3\mathbf{p}/(2\pi)^3$ and

$$\begin{aligned}\left[\mathbf{a}_i(\mathbf{p}), \mathbf{a}_k^{\dagger}(\mathbf{p}')\right] &= (2\pi)^3\delta^3(\mathbf{p}-\mathbf{p}')\delta_{ik}, \\ \left[\mathbf{b}_i(\mathbf{p}), \mathbf{b}_k^{\dagger}(\mathbf{p}')\right] &= (2\pi)^3\delta^3(\mathbf{p}-\mathbf{p}')\delta_{ik}. \end{aligned} \tag{3.5}$$

The two-particle states of zero total charge are defined by

$$\begin{aligned}|\,\mathbf{p}_1,\mathbf{p}_2\rangle_+ &= \mathbf{a}_-^{\dagger}(\mathbf{p}_1)\mathbf{b}_+^{\dagger}(\mathbf{p}_2)\,|0\rangle, \\ |\,\mathbf{p}_3,\mathbf{p}_4\rangle_0 &= \mathbf{a}_0^{\dagger}(\mathbf{p}_3)\mathbf{b}_0^{\dagger}(\mathbf{p}_4)\,|0\rangle, \end{aligned} \tag{3.6}$$

and the total and reduced masses Σ_i and μ_i, respectively, read

$$\Sigma_i = M_{\pi^i} + M_{K^i}, \quad \mu_i = \frac{M_{\pi^i}M_{K^i}}{M_{\pi^i}+M_{K^i}}, \quad i = +, 0. \tag{3.7}$$

3.2 Master equation

To evaluate the decay width and the strong energy shifts we make use of resolvents. This technique, which was developed by Feshbach a long time ago [47], has been discussed extensively in [23]. To remove the center of mass momentum from the matrix elements of any operators $\mathbf{R}$, we introduce the notation

$$\begin{aligned}{}_a\langle\mathbf{p}_1,\mathbf{p}_2|\,\mathbf{R}(z)\,|\mathbf{p}_3,\mathbf{p}_4\rangle_b = & (2\pi)^3\delta^3(\mathbf{p}_1+\mathbf{p}_2-\mathbf{p}_3-\mathbf{p}_4) \\ & \times {}_a(\mathbf{p}_1,\mathbf{p}_2|\,\mathbf{R}(z)\,|\mathbf{p}_3,\mathbf{p}_4)_b, \end{aligned} \tag{3.8}$$

where a, b stand for $0, +$. Further, we have

$${}_a(\mathbf{q},-\mathbf{q}|\,\mathbf{R}(z)\,|\mathbf{p},-\mathbf{p})_b \doteq {}_a(\mathbf{q}|\,\mathbf{R}(z)\,|\mathbf{p})_b. \tag{3.9}$$

The master formula to be solved is given by the following eigenvalue equation:

$$z - E_n - \int \mathrm{d}\nu(\mathbf{P})\langle\Psi_{n0},\mathbf{P}|\,\bar{\boldsymbol{\tau}}(z)\,|\Psi_{n0},0\rangle = 0, \tag{3.10}$$

where $E_n = \Sigma_+ - \alpha^2\mu_+/(2n^2)$ denotes the nth Coulomb energy and the unperturbed nth eigenstate is given by

$$\begin{aligned}&|\Psi_{n0},\mathbf{P}\rangle \\ &\quad = \int \mathrm{d}\nu(\mathbf{q})\Psi_{n0}(\mathbf{q})\left|\frac{\mu_+}{M_{K^+}}\mathbf{P}+\mathbf{q}, \frac{\mu_+}{M_{\pi^+}}\mathbf{P}-\mathbf{q}\right\rangle_+ . \end{aligned} \tag{3.11}$$

Here $\Psi_{n0}(\mathbf{q})$ stands for the Coulomb wave function of the bound $\pi^{\pm}K^{\mp}$ system in momentum space. The operator $\bar{\boldsymbol{\tau}}$, defined through

$$\bar{\boldsymbol{\tau}} = \mathbf{V} + \mathbf{V}\bar{\mathbf{G}}_{\rm C}^n\bar{\boldsymbol{\tau}}, \quad \mathbf{V} = \mathbf{H}_{\rm D} + \mathbf{H}_{\rm S}, \tag{3.12}$$

is regular in the vicinity of E_n. The quantity $\bar{\mathbf{G}}_{\rm C}^n$ stands for the nth energy eigenstate singularity removed Coulomb resolvent,

$$\begin{aligned}\bar{\mathbf{G}}_{\rm C}^n &= \mathbf{G}_{\rm C}\left\{\mathbf{1} - \int \mathrm{d}\nu(\mathbf{P})\,|\Psi_{n0},\mathbf{P}\rangle\langle\Psi_{n0},\mathbf{P}|\right\}, \\ \mathbf{G}_{\rm C} &= \frac{1}{z-\mathbf{H}_0-\mathbf{H}_{\rm C}}. \end{aligned} \tag{3.13}$$

The master equation presents a compact form of the Rayleigh–Schrödinger perturbation theory. If we insert $\bar{\boldsymbol{\tau}}$ iteratively into (3.10), the eigenvalue equation becomes

$$z = E_n - |\Psi_{n0}(\mathbf{x}=0)|^2\left[C_1 + C_2^2 J_0(z)\right] + \cdots, \tag{3.14}$$

where $\Psi_{n0}(\mathbf{x}=0)$ stands for the Coulomb wave function in coordinate space and J_0 denotes the loop integral in (D.3). The function J_0 is analytic in the complex z plane, except for a cut on the real axis starting at $z = \Sigma_0$. The imaginary part of J_0 has the same sign as $\mathrm{Im}\,z$ throughout the cut z plane, which does not allow (3.14) to have a solution on the first Riemann sheet. However, if we analytically continue J_0 from the upper rim of the cut to the second Riemann sheet, we find a solution at $z = \mathrm{Re}\,z + \mathrm{i}\,\mathrm{Im}\,z$, with

$$\begin{aligned}\mathrm{Re}\, z &= E_n - \frac{\alpha^3\mu_+^3 C_1}{\pi n^3} + \cdots,\\ \mathrm{Im}\, z &= -\frac{\alpha^3\mu_+^3\mu_0}{2\pi^2 n^3} C_2^2\sqrt{\rho_n} + \cdots,\end{aligned} \tag{3.15}$$

and $\rho_n = 2\mu_0\,(E_n - \Sigma_0)$. In the following, we evaluate the S-wave decay width $\Gamma_{n0} = -2\mathrm{Im}\, z$ at order $\delta^{9/2}$ and the energy shift $\Delta E_{n0} = \mathrm{Re}\, z - E_n$ at order δ^4. We focus on the strong part of the energy shift only; the evaluation of the electromagnetic energy shift is discussed in Sect. 5.1. As in [23], we reduce (3.10) to a one-channel problem with an effective potential $\mathbf{W}$,

$$\varrho\bar{\boldsymbol{\tau}}\varrho = \varrho\mathbf{W}\varrho + \varrho\mathbf{W}\varrho\bar{\mathbf{G}}_{\mathrm{C}}^n\varrho\bar{\boldsymbol{\tau}}\varrho, \tag{3.16}$$

where

$$\mathbf{W} = \mathbf{V} + \mathbf{V}\varrho_0\bar{\mathbf{G}}_{\mathrm{C}}^n\left\{\mathbf{1} - \varrho_0\mathbf{V}\varrho_0\bar{\mathbf{G}}_{\mathrm{C}}^n\right\}^{-1}\varrho_0\mathbf{V}. \tag{3.17}$$

Here ϱ (ϱ_0) denotes the charged (neutral) two-particle projector

$$\begin{aligned}\varrho &= \int \mathrm{d}\nu(\mathbf{p}_1)\mathrm{d}\nu(\mathbf{p}_2)\;|\,\mathbf{p}_1,\mathbf{p}_2\rangle_{++}\langle\mathbf{p}_1,\mathbf{p}_2\,|,\\ \varrho_0 &= \mathbf{1} - \varrho.\end{aligned} \tag{3.18}$$

The matrix element of $\mathbf{W}$ between charged states takes the form[2]

$$\begin{aligned}{}_+\langle\mathbf{q}|\,\mathbf{W}(z)\,|\mathbf{p}\rangle_+ &= (2\pi)^3\delta^3(\mathbf{q}-\mathbf{p})\\ &\times\left[-\frac{\mathbf{p}^4}{8}\left(\frac{1}{M_{\pi^+}^3}+\frac{1}{M_{K^+}^3}\right)+\cdots\right] + w(z) + w_1(z)\mathbf{p}^2\\ &+ w_2(z)\mathbf{q}^2 + w_3(z)\mathbf{p}\mathbf{q} + \cdots\end{aligned} \tag{3.19}$$

To the accuracy we are working in, only the constant term $w(z)$ contributes to the decay width and strong energy shift. We get for the S-wave decay width of the π^-K^+ atom at order $\delta^{9/2}$

$$\begin{aligned}\Gamma_{n0} &= -2\,|\Psi_{n0}(\mathbf{x}=0)|^2\,\mathrm{Im}\, w(E_n)\\ &\times(1 + 2\mathrm{Re}\, w(E_n)\langle\bar{\mathbf{g}}_{\mathrm{C}}^n(E_n)\rangle) + \mathcal{O}(\delta^5),\end{aligned} \tag{3.20}$$

while the S-wave energy-level shifts due to strong interactions read at order δ^4,

$$\begin{aligned}\Delta E_{n0}^{\mathrm{h}} &= |\Psi_{n0}(\mathbf{x}=0)|^2\mathrm{Re}\, w(E_n)\\ &\times(1 + \mathrm{Re}\, w(E_n)\langle\bar{\mathbf{g}}_{\mathrm{C}}^n(E_n)\rangle) + \mathcal{O}(\delta^5).\end{aligned} \tag{3.21}$$

The quantity $\langle\bar{\mathbf{g}}_{\mathrm{C}}^n(E_n)\rangle$, given in Appendix C, is related to the integrated Schwinger Green function [48]. The real and imaginary part of $w(z)$ are given by

$$\begin{aligned}\mathrm{Re}\, w(E_n) &= -C_1 + \frac{C_2^2 C_3\mu_0^2}{4\pi^2}\rho_n,\\ \mathrm{Im}\, w(E_n) &= -\frac{\mu_0\sqrt{\rho_n}}{2\pi}C_2^2\\ &\times\left[1 - \frac{C_3^2\mu_0^2\rho_n}{4\pi^2} + \frac{5\mu_0\rho_n}{8}\frac{M_{\pi^0}^3 + M_{K^0}^3}{M_{\pi^0}^3 M_{K^0}^3}\right]\end{aligned} \tag{3.22}$$

The decay width (3.20) and energy shift (3.21) still depend on the effective couplings C_i, which have to be related to physical quantities.

[2] The delta function term contributes to the electromagnetic energy shift; see (5.6).

3.3 Matching procedure

We now determine the diverse couplings from matching the non-relativistic and the relativistic amplitudes at threshold. With the effective Lagrangian in (A.2), (A.4) and (A.5) we may calculate the non-relativistic $\pi^-K^+ \to \pi^0K^0$ and $\pi^-K^+ \to \pi^-K^+$ scattering amplitudes at threshold at order δ. Again, we may omit contributions from transverse photons. The radiative corrections to the one-particle irreducible amplitudes, generated by transverse photons, vanish at threshold at order e^2.

The coupling C_3 enters the decay width (3.20) at order $\delta^{9/2}$ and the energy shift (3.21) at order δ^4 and is therefore needed at $\mathcal{O}(\delta^0)$ only. However, we have to determine both C_1 and C_2 at next-to-leading order in isospin symmetry breaking. The relativistic amplitudes are related to the non-relativistic ones through

$$T_{\mathrm{R}}^{lm;ik}(\mathbf{q};\mathbf{p}) = 4\,[\omega_i(\mathbf{p})\omega_k(\mathbf{p})\omega_l(\mathbf{q})\omega_m(\mathbf{q})]^{\frac{1}{2}}\,T_{\mathrm{NR}}^{lm;ik}(\mathbf{q};\mathbf{p}), \tag{3.23}$$

where $\omega_i(\mathbf{p}) = (M_i^2+\mathbf{p}^2)^{1/2}$ and $\mathbf{p}$, ($\mathbf{q}$) denotes the incoming (outgoing) relative 3-momentum. In the isospin symmetry limit, only the lowest order of the non-relativistic Lagrangian contributes at threshold and the effective couplings C_1, C_2 and C_3 yield

$$\begin{aligned}C_1 &= \frac{2\pi}{\mu_+}\left(a_0^+ + a_0^-\right), \quad C_2 = -\frac{2\sqrt{2}\pi}{\mu_+}a_0^-,\\ C_3 &= \frac{2\pi}{\mu_+}a_0^+,\end{aligned} \tag{3.24}$$

where a_0^+ and a_0^- denote the isospin even and odd S-wave scattering lengths, the notation used is specified in Appendix B. The πK scattering lengths are defined in QCD, at $m_u = m_d = \hat{m}$ and $M_\pi \doteq M_{\pi^+}$, $M_K \doteq M_{K^+}$.

To match the coupling C_2 including isospin symmetry breaking effects, we calculate the real part of the non-relativistic $\pi^-K^+ \to \pi^0K^0$ scattering matrix element in the vicinity of the threshold at order δ. In absence of virtual photons, the real part of the amplitude at threshold reads

$$\mathrm{Re}\, T_{\mathrm{NR}}^{00;\pm}(\mathbf{q};\mathbf{p}) = C_2 + C_2C_3^2J_0(\Sigma_+)^2 + \cdots \tag{3.25}$$

The ellipsis denotes terms which vanish at threshold or are of higher order in the parameter δ. The one-loop integral J_0 is given in Appendix D. Bubbles with mass insertions and/or derivative couplings do not contribute at threshold at order δ, since they contain additional factors of $\mathbf{p}^2$ and/or $\Sigma_+ - \Sigma_0$.

We now include the Coulomb interaction. Feynman graphs with a Coulomb photon attached such that the heavy fields must propagate in time to connect the two vertices all vanish. This is because we may close the integration contour over the zero-component of the loop momentum in the half-plane where there is no singularity in the propagators. One example is the self-energy diagram, which vanishes at order α. As a result of this, there is no mass renormalization in the non-relativistic theory and the mass parameters M_{π^i} and M_{K^i}, $i = 0, +$ in the

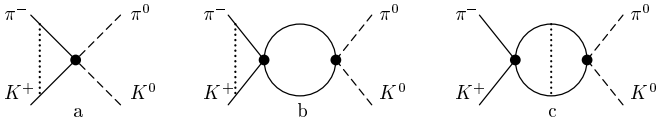

Fig. 1. One-photon exchange diagrams for the $\pi^- K^+ \to \pi^0 K^0$ scattering amplitude. The dotted line denotes a Coulomb photon. The dots stand for the couplings C_i, $i = 1, 2$

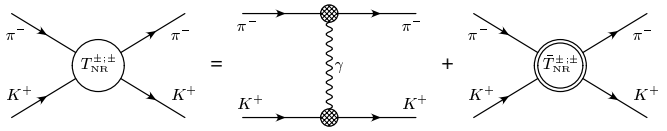

Fig. 2. Non-relativistic $\pi^- K^+ \to \pi^- K^+$ scattering amplitude. The blob describes the vector form factor of the pion and kaon. $\bar{T}^{\pm;\pm}_{\rm NR}$ denotes the truncated amplitude

non-relativistic Lagrangian (A.4) stand for the physical meson masses. The amplitude at threshold contains both infrared and ultraviolet singularities, coming from the one-Coulomb photon exchange diagrams depicted in Fig. 1. Around threshold, we get for the one-Coulomb exchange diagrams,

$$T^{00;\pm}_{\rm NR}(\mathbf{q};\mathbf{p}) = -C_2 V_{\rm C}(\mathbf{p}, P^0_{\rm thr}) \left[1 + C_1 J_+(P^0_{\rm thr})\right] + C_1 C_2 B_{\rm C}(P^0_{\rm thr}) + \cdots , \tag{3.26}$$

where $P^0_{\rm thr} = \Sigma_+ + \mathbf{p}^2/(2\mu_+)$. The Coulomb vertex function $V_{\rm C}$ in Fig. 1a and the two-loop integral $B_{\rm C}$ in Fig. 1c are given in Appendix D. The integral J_+, specified in (D.4), has to be evaluated at $d \neq 3$, because the vertex diagram generates an infrared singular Coulomb phase [49] at threshold. We split off this phase $\theta_{\rm c}$, according to

$$T^{00;\pm}_{\rm NR}(\mathbf{q},\mathbf{p}) = \mathrm{e}^{\mathrm{i}\alpha\theta_{\rm c}} \hat{T}^{00;\pm}_{\rm NR}(\mathbf{q},\mathbf{p}),$$
$$\theta_{\rm c} = \frac{\mu_+}{|\mathbf{p}|}\mu^{d-3}\left\{\frac{1}{d-3} - \frac{1}{2}\left[\ln 4\pi + \Gamma'(1)\right] + \ln\frac{2|\mathbf{p}|}{\mu}\right\}, \tag{3.27}$$

where μ denotes the running scale. The remainder $\hat{T}^{00;\pm}_{\rm NR}$ is free of infrared singularities at threshold, at order δ. We find for the real part

$$\mathrm{Re}\,\hat{T}^{00;\pm}_{\rm NR}(\mathbf{q},\mathbf{p}) = \frac{B_1}{|\mathbf{p}|} + B_2 \ln\frac{|\mathbf{p}|}{\mu_+} + \frac{1}{N}\mathrm{Re}\,A^{00;\pm}_{\rm thr} + \mathcal{O}(\mathbf{p}), \tag{3.28}$$

with

$$B_1 = C_2\frac{\alpha\pi\mu_+}{2} + o(\delta), \quad B_2 = -C_1 C_2 \frac{\alpha\mu_+^2}{\pi} + o(\delta), \tag{3.29}$$

and

$$N = 4M_{\pi^+}M_{K^+} + \frac{M_{K^+} - M_{\pi^+}}{M_{K^+} + M_{\pi^+}}\left(\Delta_K - \Delta_\pi\right). \tag{3.30}$$

At order δ, the constant term in (3.28) reads

$$\frac{1}{N}\mathrm{Re}\,A^{00;\pm}_{\rm thr} = C_2\left\{1 - C_3^2\frac{\mu_0^3(\Sigma_+ - \Sigma_0)}{2\pi^2} + C_1\frac{\alpha\mu_+^2}{2\pi}\left[1 - \Lambda(\mu) - \ln\frac{4\mu_+^2}{\mu^2}\right]\right\} + o(\delta). \tag{3.31}$$

The ultraviolet divergence $\Lambda(\mu)$, given in (C.5), stems from the two-loop diagram $B_{\rm C}$ and may be absorbed in the renormalization of the coupling C_2,

$$C_2^{\rm r}(\mu) = C_2\left[1 - \frac{\alpha\mu_+^2}{2\pi}C_1\Lambda(\mu)\right]. \tag{3.32}$$

We now determine the coupling constant C_1. At $\alpha = 0$, the real part of the non-relativistic $\pi^- K^+ \to \pi^- K^+$ scattering amplitude reads at threshold

$$\mathrm{Re}\,T^{\pm;\pm}_{\rm NR}(\mathbf{p},\mathbf{p}) = C_1 + C_3 C_2^2 J_0(\Sigma_+)^2 + \cdots , \tag{3.33}$$

where the ellipsis denotes contributions which vanish at threshold or are of $o(\delta)$. In the presence of virtual photons, we first have to subtract the one-photon exchange diagram from the full amplitude, as displayed in Fig. 2. The coupling constant C_1 is now determined by the one-particle irreducible part of the amplitude. The truncated part $\bar{T}^{\pm;\pm}_{\rm NR}$ again contains one-photon exchange diagrams as shown in Fig. 3,

$$\bar{T}^{\pm;\pm}_{\rm NR}(\mathbf{p},\mathbf{p}) = -2C_1 V_{\rm C}(\mathbf{p}, P^0_{\rm thr})\left[1 + C_1 J_+(P^0_{\rm thr})\right] + C_1^2 B_{\rm C}(P^0_{\rm thr}) + \cdots \tag{3.34}$$

All diagrams with a Coulomb photon exchange between an incoming and an outgoing particle vanish, because the pions (kaons) must propagate in time in order to connect the two vertices. Again the vertex function $V_{\rm C}$ leads to an infrared singular Coulomb phase at threshold,

$$\bar{T}^{\pm;\pm}_{\rm NR}(\mathbf{p},\mathbf{p}) = \mathrm{e}^{2\mathrm{i}\alpha\theta_{\rm c}}\hat{T}^{\pm;\pm}_{\rm NR}(\mathbf{p},\mathbf{p}), \tag{3.35}$$

where $\hat{T}^{\pm;\pm}_{\rm NR}$ is free of infrared singularities at threshold at order δ. Further, the real part of the infrared regular amplitude $\hat{T}^{\pm;\pm}_{\rm NR}$ is given by

$$\mathrm{Re}\,\hat{T}^{\pm;\pm}_{\rm NR}(\mathbf{p},\mathbf{p}) = \frac{B_1'}{|\mathbf{p}|} + B_2' \ln\frac{|\mathbf{p}|}{\mu_+}$$

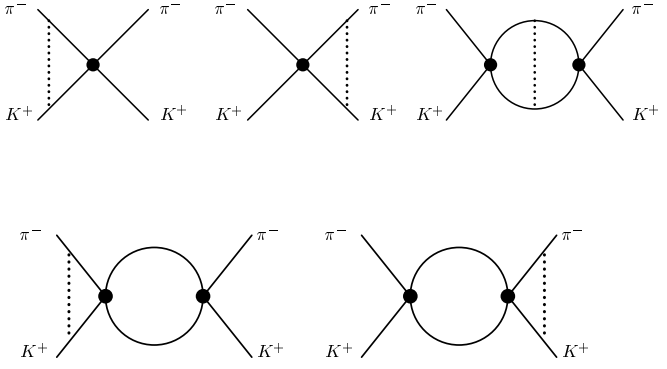

Fig. 3. One-photon exchange diagrams for the truncated $\pi^- K^+ \to \pi^- K^+$ scattering amplitude. The dotted line denotes a Coulomb photon. The dot denotes the coupling C_2

$$+\frac{1}{4M_{\pi^+}M_{K^+}}\mathrm{Re}\,A_{\mathrm{thr}}^{\pm;\pm}+\mathcal{O}(\mathbf{p}), \qquad (3.36)$$

with

$$B_1'=C_1\alpha\pi\mu_+ +o(\delta),\quad B_2'=-\frac{C_1^2\alpha\mu_+^2}{\pi}+o(\delta), \qquad (3.37)$$

and

$$\begin{aligned}&\frac{1}{4M_{\pi^+}M_{K^+}}\mathrm{Re}\,A_{\mathrm{thr}}^{\pm;\pm}\\&=C_1\left\{1+\frac{C_1\alpha\mu_+^2}{2\pi}\left[1-\Lambda(\mu)-\ln\frac{4\mu_+^2}{\mu^2}\right]\right\}\\&\quad-\frac{C_2^2C_3\mu_0^3}{2\pi^2}(\Sigma_+-\Sigma_0)+o(\delta).\end{aligned} \qquad (3.38)$$

Here, the ultraviolet pole term $\Lambda(\mu)$ in B_{C} is removed by renormalizing the coupling C_1, according to

$$C_1^{\mathrm{r}}(\mu)=C_1\left[1-\frac{\alpha\mu_+^2}{2\pi}C_1\Lambda(\mu)\right]. \qquad (3.39)$$

The above renormalization of the low-energy couplings C_1 and C_2 eliminates at the same time the ultraviolet divergences contained in the expressions for the decay width (3.20) and the energy shift (3.21). We assume that the relativistic πK amplitudes at order δ have the same singularity structure as the non-relativistic amplitudes and use (3.23) to match the non-relativistic expressions to the relativistic ones. The calculations of the relativistic $\pi^-K^+\to\pi^0K^0$ and $\pi^-K^+\to\pi^-K^+$ scattering amplitudes have been performed at $\mathcal{O}(p^4,e^2p^2)$ in [36,50,51]. Both the Coulomb phase and the singular term $\sim\ln|\mathbf{p}|$ are absent in the real part of the amplitudes at this order of accuracy; they first occur at order e^2p^4. The quantity $\mathrm{Re}\,A_{\mathrm{thr}}^{00;\pm}$ ($\mathrm{Re}\,A_{\mathrm{thr}}^{\pm;\pm}$) is determined by the constant term occurring in the threshold expansion of the corresponding relativistic amplitude. Further, the relativistic calculations [36,50,51], contain the same singular contribution $\sim 1/|\mathbf{p}|$ as the non-relativistic amplitude in (3.28) and (3.36).

The results for the matching of the coupling constants $C_1^{\mathrm{r}}(\mu)$ and $C_2^{\mathrm{r}}(\mu)$ yield at next-to-leading order in isospin symmetry breaking,

$$\begin{aligned}C_2^{\mathrm{r}}(\mu)=\frac{1}{N}\mathrm{Re}\,A_{\mathrm{thr}}^{00;\pm}-2\sqrt{2}\pi a_0^-\big[&2(\Sigma_+-\Sigma_0)(a_0^+)^2\\&+\alpha\left(\ln\frac{4\mu_+^2}{\mu^2}-1\right)(a_0^++a_0^-)\Big],\end{aligned} \qquad (3.40)$$

and

$$\begin{aligned}C_1^{\mathrm{r}}(\mu)=\frac{1}{4M_{\pi^+}M_{K^+}}\mathrm{Re}\,A_{\mathrm{thr}}^{\pm;\pm}&+8\pi(\Sigma_+-\Sigma_0)a_0^+(a_0^-)^2\\&+2\pi\alpha\left(\ln\frac{4\mu_+^2}{\mu^2}-1\right)(a_0^++a_0^-)^2.\end{aligned} \qquad (3.41)$$

4 Strong energy shift and width

The matching relations in Sect. 3.3 allow us to specify the results for the decay width and the strong energy shift in terms of the relativistic πK scattering amplitudes at threshold. The expressions are valid at next-to-leading order in isospin symmetry breaking, and to all orders in the chiral expansion.

4.1 S-wave decay width of the πK atom

The matching results in (3.24) and (3.40) yield for the decay width at order $\delta^{9/2}$ in terms of the relativistic $\pi^-K^+\to\pi^0K^0$ amplitude at threshold,

$$\begin{aligned}\Gamma_{n0}&=\frac{8\alpha^3\mu_+^2}{n^3}p_n^*\mathcal{A}^2\,(1+K_n)\,,\\\mathcal{A}&=-\frac{1}{8\sqrt{2}\pi}\frac{1}{\Sigma_+}\mathrm{Re}\,A_{\mathrm{thr}}^{00;\pm}+o(\delta),\end{aligned} \qquad (4.1)$$

where

$$\begin{aligned}K_n=&\frac{M_{\pi^+}\Delta_K+M_{K^+}\Delta_\pi}{M_{\pi^+}+M_{K^+}}(a_0^+)^2\\&-4\alpha\mu_+(a_0^++a_0^-)\left[\psi(n)-\psi(1)-\frac{1}{n}+\ln\frac{\alpha}{n}\right]+o(\delta)\end{aligned} \qquad (4.2)$$

and $\psi(n)=\Gamma'(n)/\Gamma(n)$. Aside from the kinematical factor p_n^*, the decay width is expanded in powers of α and m_u-m_d. The outgoing relative 3-momentum

$$p_n^*=\frac{1}{2E_n}\lambda\left(E_n^2,M_{\pi^0}^2,M_{K^0}^2\right)^{1/2}, \qquad (4.3)$$

with $\lambda(x,y,z)=x^2+y^2+z^2-2xy-2xz-2yz$, is chosen such that the total final state energy corresponds to the nth energy eigenvalue of the π^-K^+ atom. In the isospin limit, the $\pi^-K^+\to\pi^0K^0$ amplitude at threshold is determined by the isospin odd scattering length a_0^-. In order to extract a_0^- from the above result of the decay width, we first have to subtract the isospin breaking contribution from the amplitude. We expand the normalized amplitude in powers of the isospin breaking parameter δ,

$$\mathcal{A}=a_0^-+\epsilon+o(\delta). \qquad (4.4)$$

The isospin breaking corrections ϵ have been evaluated at $\mathcal{O}(p^4,e^2p^2)$ in [50,51]. See also the comments in Sect. 7. We may now rewrite the expression for the width in the following form:

$$\begin{aligned}\Gamma_{n0}&=\frac{8\alpha^3\mu_+^2}{n^3}p_n^*(a_0^-)^2\,(1+\delta_{K,n})+\mathcal{O}(\delta^5),\\\delta_{K,n}&=\frac{2\epsilon}{a_0^-}+K_n.\end{aligned} \qquad (4.5)$$

The corrections $\delta_{K,n}$ to the Deser-type formula have been worked out at order α, m_u-m_d, $\alpha\hat{m}$ and $(m_u-m_d)\hat{m}$.

Table 1. Next-to-leading order corrections to the Deser-type formulae

	$10^2\delta_{h,1}$	$10^2\delta_{h,2}$	$10^2\delta'_{h,1}$	$10^2\delta'_{h,2}$
$\pi^+\pi^-$ atom	5.8 ± 1.2	5.6 ± 1.2	6.2 ± 1.2	6.1 ± 1.2
$\pi^\pm K^\mp$ atom	4.0 ± 2.2	3.8 ± 2.2	1.7 ± 2.2	1.5 ± 2.2

The corrections $\delta_{K,n}$, where $n = 1, 2$ are given numerically in Table 1.

For the P-wave decay width into $\pi^0 K^0$, the leading order term is proportional the square of the coupling C_7 and of order $\delta^{13/2}$. After performing the matching, we get at leading order

$$\Gamma_{n1,\pi^0K^0} = \frac{8(n^2-1)}{n^5}\alpha^5\mu_+^4 {p_n^*}^3 \left(a_1^-\right)^2, \tag{4.6}$$

where a_1^- denotes the P-wave scattering length.

4.2 Strong energy shift of the πK atom

With the matching results in (3.24) and (3.41), we may specify the S-wave energy shifts at order δ^4, in terms of the relativistic truncated $\pi^- K^+ \to \pi^- K^+$ amplitude at threshold,

$$\begin{aligned} \Delta E_{n0}^{\rm h} &= -\frac{2\alpha^3\mu_+^2}{n^3}\mathcal{A}'\left(1 + K'_n\right), \\ \mathcal{A}' &= \frac{1}{8\pi\Sigma_+}\mathrm{Re}\, A_{\rm thr}^{\pm;\pm} + o(\delta), \end{aligned} \tag{4.7}$$

with

$$\begin{aligned} K'_n = -2\alpha\mu_+(a_0^+ + a_0^-)\left[\psi(n) - \psi(1) - \frac{1}{n} + \ln\frac{\alpha}{n}\right] \\ + o(\delta). \end{aligned} \tag{4.8}$$

For the ground state, the result agrees with the one obtained for the strong energy shift in pionic hydrogen [25], if we replace μ_+ with the reduced mass of the $\pi^- p$ atom and $\mathrm{Re}\, A_{\rm thr}^{\pm;\pm}$ with the regular part of the $\pi^- p$ amplitude at threshold.

In the isospin limit, the normalized amplitude $\mathcal{A}'$ reduces to the sum of the isospin even and odd scattering lengths $a_0^+ + a_0^-$. Again, we expand $\mathcal{A}'$ in powers of α and $m_u - m_d$,

$$\mathcal{A}' = a_0^+ + a_0^- + \epsilon' + o(\delta). \tag{4.9}$$

The corrections ϵ' have been evaluated at $\mathcal{O}(p^4, e^2p^2)$ in [36,51]. See also the comments in Sect. 7. The isospin breaking corrections to the Deser-type formula read at next-to-leading order:

$$\begin{aligned} \Delta E_{n0}^{\rm h} &= -\frac{2\alpha^3\mu_+^2}{n^3}(a_0^+ + a_0^-)\left(1 + \delta'_{K,n}\right) + \mathcal{O}(\delta^5), \\ \delta'_{K,n} &= \frac{\epsilon'}{a_0^+ + a_0^-} + K'_n, \end{aligned} \tag{4.10}$$

where $\delta'_{K,n}$ has been worked out at order α, $m_u - m_d$, $\alpha\hat{m}$ and $(m_u - m_d)\hat{m}$ in the chiral expansion. For the first two energy levels, the numerical values for $\delta'_{K,n}$ are given in Table 1. As concerns the energy splittings for $l = 1$ and $n \geq 2$, the leading order contribution is given by

$$\Delta E_{n1}^{\rm h} = -2C_6 \nabla\Psi_{n1}^*(\mathbf{x} = 0)\nabla\Psi_{n1}(\mathbf{x} = 0). \tag{4.11}$$

Here Ψ_{n1} denotes the Coulomb wave function with angular momentum $l = 1$. The low-energy coupling constant C_6 is determined through the $l = 1$ partial wave contribution to the relativistic $\pi^- K^+ \to \pi^- K^+$ scattering amplitude and we find for the energy shift,

$$\Delta E_{n1}^{\rm h} = -\frac{2(n^2-1)}{n^5}\alpha^5\mu_+^4\left(a_1^+ + a_1^-\right). \tag{4.12}$$

The result is proportional to the combination $a_1^+ + a_1^-$ of P-wave scattering lengths and suppressed by a factor of α^5.

4.3 Pionium

For pionium, we adopt the convention used in [23,30] and count α and $(m_u - m_d)^2$ as small isospin breaking parameters of order δ. The decay width and energy shifts of the $\pi^+\pi^-$ atom can be obtained from the formulae (3.20), (3.21) and (4.11) through the following substitutions of the masses $M_{K^+} \to M_{\pi^+}, M_{K^0} \to M_{\pi^0}$ and coupling constants[3]:

$$\begin{aligned} &C_1 \to c_1, \quad C_2 \to \sqrt{2}(c_2 - 2c_4\Delta_\pi), \\ &C_3 \to 2c_3, \quad C_6 \to c_6. \end{aligned} \tag{4.13}$$

The factor 2 in substituting C_3 comes from the different normalization of the $\pi^0\pi^0$ state $|\mathbf{p}_3, \mathbf{p}_4\rangle_0 = a_0^\dagger(\mathbf{p}_3)a_0^\dagger(\mathbf{p}_4)|0\rangle$. For the coupling constant C_2, the substitution is non-trivial because our basis of operators with two space derivatives differs from the one used in [23,30]. See also the comment in Sect. 3.1. The result for the S-wave decay width of pionium reads at order $\delta^{9/2}$

$$\begin{aligned} \Gamma_{\pi,n0} &= \frac{2}{9n^3}\alpha^3 p_{\pi,n}^* \mathcal{A}_\pi^2\left(1 + K_{\pi,n}\right), \\ \mathcal{A}_\pi &= a_0^0 - a_0^2 + \epsilon_\pi + o(\delta), \end{aligned} \tag{4.14}$$

where

$$\begin{aligned} K_{\pi,n} &= \frac{\kappa}{9}\left(a_0^0 + 2a_0^2\right)^2 \\ &\quad - \frac{2\alpha}{3}\left(2a_0^0 + a_0^2\right)\left[\psi(n) - \psi(1) - \frac{1}{n} + \ln\frac{\alpha}{n}\right] + o(\delta), \\ p_{\pi,n}^* &= \left(\Delta_\pi - \frac{\alpha^2}{4n^2}M_{\pi^+}^2\right)^{1/2}, \end{aligned} \tag{4.15}$$

and $\kappa = M_{\pi^+}^2/M_{\pi^0}^2 - 1$. The quantity $\mathcal{A}_\pi$ is defined as in [23,30]. The isospin symmetry breaking contributions ϵ_π have been evaluated at $\mathcal{O}(p^4, e^2p^2)$ in [23,30,52]. The corrections ϵ_π are of the order of α and $\alpha\hat{m}$. This is due to

[3] The c_i are the low-energy constants occurring in [23,30].

the fact that in the $\pi^+\pi^- \to \pi^0\pi^0$ scattering amplitude at threshold, the quark mass difference shows up at order $(m_u - m_d)^2\hat{m}$ only. For the decay width of the ground state at order $\delta^{9/2}$, we reproduce the result obtained in [20,23, 30]. Again we may rewrite the formula for the width:

$$\begin{aligned} \Gamma_{\pi,n0} &= \frac{2\alpha^3}{9n^3} p^*_{\pi,n} (a_0^0 - a_0^2)^2 \left(1 + \delta_{\pi,n}\right) + \mathcal{O}(\delta^5), \\ \delta_{\pi,n} &= \frac{2\epsilon_\pi}{a_0^0 - a_0^2} + K_{\pi,n}. \end{aligned} \tag{4.16}$$

The parameter $\delta_{\pi,n}$ contains the isospin breaking corrections to the Deser-type formula at next-to-leading order. The numerical values for $\delta_{\pi,n}$, with $n = 1, 2$ are listed in Table 1. The decay width of the P-states into a pair of two neutral pions is forbidden by C invariance.

The strong energy shift of the $\pi^+\pi^-$ atom at order δ^4 yields

$$\begin{aligned} \Delta E^{\mathrm{h}}_{\pi,n0} &= -\frac{\alpha^3 M_{\pi^+}}{n^3} \mathcal{A}'_\pi \left(1 + K'_{\pi,n}\right), \\ \mathcal{A}'_\pi &= \frac{1}{6}\left(2a_0^0 + a_0^2\right) + \epsilon'_\pi, \\ K'_{\pi,n} &= -\frac{\alpha}{3}\left(2a_0^0 + a_0^2\right)\left[\psi(n) - \psi(1) - \frac{1}{n} + \ln\frac{\alpha}{n}\right] \\ &\quad + o(\delta), \end{aligned} \tag{4.17}$$

where $\mathcal{A}'_\pi$ is defined analogously to the quantity $\mathcal{A}'$ discussed in Sect. 4.2. The isospin symmetry breaking contributions ϵ'_π have been calculated at $\mathcal{O}(p^4, e^2p^2)$ in [53,54]. Again the corrections ϵ'_π are of order α and $\alpha\hat{m}$. At order δ^4, the Deser-type formula is changed by isospin breaking corrections, according to

$$\begin{aligned} \Delta E^{\mathrm{h}}_{\pi,n0} &= -\frac{\alpha^3 M_{\pi^+}}{6n^3}(2a_0^0 + a_0^2)\left(1 + \delta'_{\pi,n}\right) + \mathcal{O}(\delta^5), \\ \delta'_{\pi,n} &= \frac{6\epsilon'_\pi}{2a_0^0 + a_0^2} + K'_{\pi,n}. \end{aligned} \tag{4.18}$$

For the first two energy levels, the numerical values for $\delta'_{\pi,n}$ are given in Table 1. Finally, the leading order contribution to the strong energy-level shift for $l = 1$ and $n \geq 2$ reads

$$\Delta E^{\mathrm{h}}_{\pi,n1} = -\frac{(n^2-1)}{8n^5}\alpha^5 M^3_{\pi^+} a_1^1, \tag{4.19}$$

where a_1^1 denotes the P-wave $\pi\pi$ scattering length.

5 Transverse photons

We now concentrate on the contributions coming from transverse photons. At order δ^4, the energy-level shifts in $\pi^+\pi^-$ and $\pi^\pm K^\mp$ atoms contain apart from the strong energy shift also an electromagnetic contribution as well as finite size effects due to the electromagnetic form-factors of the pion and kaon. We further discuss the contributions from transverse photons to the decay width of the $\pi^- K^+$ atom and show that they do not contribute at order $\delta^{9/2}$. For pionium, the various higher order decay channels have been discussed in [23].

5.1 Electromagnetic energy-level shifts

As mentioned in Sect. 2, we split the total energy shift ΔE_{nl} in (2.1) into the strong part displayed in (4.7) and an electromagnetic contribution $\Delta E^{\mathrm{em}}_{nl}$. The electromagnetic part is of order α^4 and contains both pure QED corrections as well as finite size effects due to the charge radii of the pion and kaon; see Appendix A. The energy shift contributions due to pure QED have been evaluated by the use of the Bethe–Salpeter equation [40], the quasipotential approach [41,42] and an improved Coulomb potential [43]. Nevertheless, we find it useful to provide the calculation within the non-relativistic framework.

Again, we start with the master equation (3.10), but instead of the effective potential $\mathbf{W}$, we consider the operator $\bar{\boldsymbol{\tau}}$ in the second iterative approximation,

$$\bar{\boldsymbol{\tau}} = \mathbf{V} + \mathbf{V}\bar{\mathbf{G}}^n_{\mathrm{C}}\mathbf{V} + \mathcal{O}(\mathbf{V}^3). \tag{5.1}$$

The non-relativistic Lagrangian including transverse photons (A.2), (A.4) and (A.5) gives rise to the following perturbation:

$$\begin{aligned} \mathbf{V} &= \mathbf{H}_{\mathrm{D}} + \mathbf{H}_{\mathrm{S}} + e\mathbf{H}_\gamma + e^2\lambda\mathbf{H}_\lambda, \\ \mathcal{H}_\gamma &= \mathrm{i}\mathbf{A}\left[\frac{1}{M_{\pi^+}}\pi^\dagger_-\nabla\pi_- - \frac{1}{M_{K^+}}K^\dagger_+\nabla K_+\right], \\ \mathcal{H}_\lambda &= \pi^\dagger_- K^\dagger_+ \pi_- K_+. \end{aligned} \tag{5.2}$$

The photon field $\mathbf{A}$ is given by

$$\begin{aligned} \mathbf{A}(0,\mathbf{x}) &= \int \frac{\mathrm{d}^3\mathbf{k}}{(2\pi)^3 2k^0} \\ &\times \sum_{r=1,2}\left[\boldsymbol{\epsilon}(k,r)\, a_\gamma(k,r)\mathrm{e}^{\mathrm{i}\mathbf{kx}} + \boldsymbol{\epsilon}^*(k,r) a^\dagger_\gamma(k,r)\mathrm{e}^{-\mathrm{i}\mathbf{kx}}\right], \end{aligned} \tag{5.3}$$

where $k^0 \doteq |\mathbf{k}|$ and $\boldsymbol{\epsilon}(k,r)$ denote the transversal polarization vectors. The operator a_γ satisfies the commutation relation,

$$\left[a_\gamma(k,r), a^\dagger_\gamma(k',r')\right] = 2k^0(2\pi)^3\delta^3(\mathbf{k}-\mathbf{k}')\delta_{rr'}, \tag{5.4}$$

and the one-photon states read

$$|\mathbf{k}, r\rangle = a^\dagger_\gamma(k,r)|0\rangle. \tag{5.5}$$

The electromagnetic contributions to the energy-level shifts consists of

$$\begin{aligned} \Delta E^{\mathrm{em}}_{nl} &= -\frac{1}{8\mu_+^3}\left(1 - \frac{3\mu_+}{\Sigma_+}\right) \\ &\times \int \mathrm{d}^3\mathbf{r}\, \Psi^*_{nl}(\mathbf{r})\Delta^2\Psi_{nl}(\mathbf{r}) + e^2\lambda|\Psi_{n0}(\mathbf{x}=0)|^2 \\ &- \int \mathrm{d}\nu(\mathbf{p})|\Psi_{nl}(\mathbf{p})|^2\left[\hat{\Sigma}_\pi(\Omega_n,\mathbf{p}) + \hat{\Sigma}_K(\Omega_n,\mathbf{p})\right] \\ &- \frac{e^2}{M_{\pi^+}M_{K^+}}\int \mathrm{d}\nu(\mathbf{p})\mathrm{d}\nu(\mathbf{p}')\Psi^*_{nl}(\mathbf{p})G_\gamma(\mathbf{p},\mathbf{p}')\Psi_{nl}(\mathbf{p}'), \end{aligned} \tag{5.6}$$

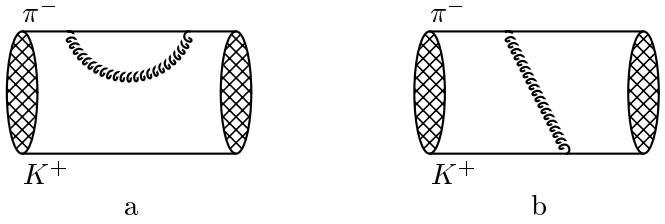

Fig. 4. Self-energy **a** and one-photon exchange contributions **b** to the electromagnetic energy shift. The twisted lines denote transverse photons

with $\Omega_n = \Sigma_+ + \mathbf{p}^2/(2\mu_+) - E_n$ and Ψ_{nl} denotes the Coulomb wave function for arbitrary n and l. Here, the first term contains the mass insertions $\mathbf{H}_{\rm D}$, the second describes the finite size effects due to $\mathbf{H}_\lambda$, while the last two terms come from the self-energy and one-photon exchange diagrams depicted in Fig. 4a,b.

To avoid contributions from hard photon momenta, we use the threshold expansion [55,56] to evaluate the self-energy contributions. This procedure is outlined in Appendix D and the threshold expanded self-energy $\hat{\Sigma}_h$, where $h = \pi, K$, is specified in (D.17). As can be read off from the wave function in momentum space, the relative 3-momentum $\mathbf{p}$ is of order δ. Hence the quantities $\hat{\Sigma}_\pi(\Omega_n, \mathbf{p})$ and $\hat{\Sigma}_K(\Omega_n, \mathbf{p})$ count as order δ^5 and are beyond the accuracy of our calculation.

What remains to be calculated is the one-photon exchange contribution[4]. The integrand

$$\begin{aligned} &G_\gamma(\mathbf{p}, \mathbf{p}') \\ &= \frac{1}{|\mathbf{p}-\mathbf{p}'|}\left[\frac{\alpha^2\mu_+}{2n^2} + \frac{\mathbf{p}^2}{2M_{\pi^+}} + \frac{\mathbf{p}'^2}{2M_{K^+}} + |\mathbf{p}-\mathbf{p}'|\right]^{-1} \\ &\quad\times\frac{1}{4}\left[(\mathbf{p}+\mathbf{p}')^2 - \frac{(\mathbf{p}^2-\mathbf{p}'^2)^2}{(\mathbf{p}-\mathbf{p}')^2}\right], \end{aligned} \tag{5.7}$$

is an inhomogeneous function in the parameter δ, and to the accuracy we are working required at leading order in δ only,

$$G_\gamma(\mathbf{p}, \mathbf{p}') = \frac{1}{4}\frac{1}{|\mathbf{p}-\mathbf{p}'|^2}\left[(\mathbf{p}+\mathbf{p}')^2 - \frac{(\mathbf{p}^2-\mathbf{p}'^2)^2}{(\mathbf{p}-\mathbf{p}')^2}\right] + \cdots \tag{5.8}$$

In order to evaluate the one-photon exchange contributions, we replace the terms $\sim \mathbf{p}^2\Psi^*_{nl}(\mathbf{p})$ and $\sim \mathbf{p}'^2\Psi_{nl}(\mathbf{p}')$ by making use of the Schrödinger equation,

$$\left[\mathbf{p}^2 + \frac{\alpha^2\mu_+^2}{n^2}\right]\Psi_{nl}(\mathbf{p}) = 8\pi\alpha\mu_+\int \mathrm{d}\nu(\mathbf{q})\frac{1}{|\mathbf{p}-\mathbf{q}|^2}\Psi_{nl}(\mathbf{q}). \tag{5.9}$$

Further, we use the Fourier transform of $|\mathbf{p}-\mathbf{p}'|^{-2}$, $|\mathbf{p}-\mathbf{q}|^{-2}$ and $|\mathbf{p}'-\mathbf{q}|^{-2}$ to express the wave functions in coordinate space. The one-photon exchange contribution now reads at order α^4,

$$\frac{\pi\alpha}{\mu_+\Sigma_+}|\Psi_{n0}(\mathbf{x}=0)|^2 + \frac{\alpha^3\mu_+}{n^2\Sigma_+}\langle r^{-1}\rangle - \frac{3\alpha^2}{2\Sigma_+}\langle r^{-2}\rangle, \tag{5.10}$$

where the expectation values are defined as

$$\langle r^{-k}\rangle = \int \mathrm{d}^3\mathbf{r}\,\Psi^*_{nl}(\mathbf{r})\frac{1}{|\mathbf{r}|^k}\Psi_{nl}(\mathbf{r}), \quad k = 1, 2. \tag{5.11}$$

The electromagnetic energy shift at order α^4 yields

$$\begin{aligned} \Delta E^{\rm em}_{nl} &= \frac{\alpha^4\mu_+}{n^3}\left(1 - \frac{3\mu_+}{\Sigma_+}\right)\left[\frac{3}{8n} - \frac{1}{2l+1}\right] \\ &+ \frac{4\alpha^4\mu_+^3\lambda}{n^3}\delta_{l0} + \frac{\alpha^4\mu_+^2}{\Sigma_+}\left[\frac{1}{n^3}\delta_{l0} + \frac{1}{n^4} - \frac{3}{n^3(2l+1)}\right] \\ &+ \mathcal{O}(\alpha^5\ln\alpha). \end{aligned} \tag{5.12}$$

Here, the first terms is generated by the mass insertions, the second one contains the finite size effects and the last one stems from the one-photon exchange contributions (5.10). For n and l arbitrary, we get the same result for the pure QED contributions as [40,41,43]. Further the formula for the ground state agrees with the result obtained in [25] for the electromagnetic energy shift of the $\pi^- p$ atom, if we replace λ by the corresponding quantity in pionic hydrogen.

To analyze the electromagnetic energy splittings of pionium, we need to construct an effective Lagrangian that describes the relativistic $\pi^+\pi^- \to \pi^+\pi^-$ amplitude at threshold correctly up to and including order α. The annihilation graph showed in Fig. 5 corresponds to a local four pion interaction in the non-relativistic Lagrangian. However, the corresponding relativistic scattering matrix element vanishes at threshold. We may thus obtain the electromagnetic energy-level shift from (5.12) by simply substituting $\mu_+ \to M_{\pi^+}/2$, $\Sigma_+ \to 2M_{\pi^+}$ and $\lambda \to 1/3\langle r^2_{\pi^+}\rangle$,

$$\begin{aligned} \Delta E^{\rm em}_{\pi,nl} &= \alpha^4 M_{\pi^+}\left[\frac{\delta_{l0}}{8n^3} + \frac{11}{64n^4} - \frac{1}{2n^3(2l+1)}\right] \\ &+ \frac{\alpha^4 M^3_{\pi^+}\langle r^2_{\pi^+}\rangle}{6n^3}\delta_{l0} + \mathcal{O}(\alpha^5\ln\alpha). \end{aligned} \tag{5.13}$$

5.2 Decay channels of the πK atom

Next we discuss the contributions from other decay channels to the decay width of the $\pi^- K^+$ atom. As already mentioned in Sect. 2, for S-states the only possible decay channels are $K^0 + n_1\gamma + n_2 e^+e^-$ and $\pi^0 K^0 + n_1\gamma + n_2 e^+e^-$, where $n_1 + n_2 > 0$. Here n_1 denotes the number of photons

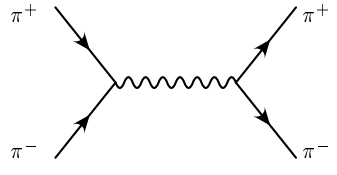

Fig. 5. Annihilation diagram $\pi^+\pi^- \to \pi^+\pi^-$ at order α in the relativistic theory

[4] We thank A. Rusetsky for a very useful communication concerning technical aspects of the calculation.

and n_2 the number of e^+e^- pairs. The decay widths into $\pi^-K^+ + n_1\gamma + n_2e^+e^-$ vanish due to lack of phase space. Moreover, radiative transitions[5] with the emission of one photon are forbidden between two states with $l = 0$. For the 2P-state of the π^-K^+ atom on the contrary, the main annihilation mechanism is the $2p$–$1s$ radiative transition into the ground state, followed by the decay into π^0K^0.

To investigate the decays into $K^0 + n\gamma$, $n = 1, 2$, we have to extend the Lagrangian in (A.4) and (A.5) to include terms with odd intrinsic parity, such as

$$\begin{aligned}\mathcal{L}_{\rm A} &= eD_1\mathbf{B}\cdot(\pi_-^\dagger \overleftrightarrow{\mathbf{D}} K_+^\dagger K_0 + \text{h.c.})\\ &\quad + e^2D_2\mathbf{E}\cdot\mathbf{B}(\pi_-^\dagger K_+^\dagger K_0 + \text{h.c.}) + \cdots, \quad (5.14)\end{aligned}$$

where $u\overleftrightarrow{\mathbf{D}}v \doteq u\mathbf{D}v - v\mathbf{D}u$. The covariant derivative $\mathbf{D}$ is specified in Appendix A, $\mathbf{E}$ denotes the electric and $\mathbf{B}$ the magnetic field. The couplings D_1 and D_2 are real and may be determined through matching with the chiral expansion of the relativistic amplitudes. In the relativistic theory, the $\pi^+K^-K^02\gamma$ vertex is contained in the Wess–Zumino–Witten term [45]. The $\pi^+K^-K^0\gamma$ interaction occurs only after inclusion of the odd intrinsic parity sector of the ChPT Lagrangian at $\mathcal{O}(p^6)$ [46]. The Hamiltonian thus extended is hermitian and the operator $\bar{\boldsymbol{\tau}}$ obeys the unitarity condition,

$$\bar{\boldsymbol{\tau}}(z) - \bar{\boldsymbol{\tau}}^\dagger(z) = -2\pi\mathrm{i}\bar{\boldsymbol{\tau}}(z)\bar{\delta}(z - \mathbf{H}_0 - \mathbf{H}_{\rm C})\bar{\boldsymbol{\tau}}^\dagger(z). \quad (5.15)$$

The symbol $\bar{\delta}$ is understood as follows: in order to evaluate the right-hand side of the equation, we insert a complete set of eigenstates $(\mathbf{H}_0 + \mathbf{H}_{\rm C})|\,\beta\rangle = E_\beta\,|\,\beta\rangle$, omitting the nth Coulomb eigenstate of the π^-K^+ atom. This implies for the total decay width

$$\Gamma_{nl} = \sum_\beta \Gamma_{nl,\beta}, \quad (5.16)$$

where

$$\begin{aligned}\Gamma_{nl,\beta} &= \int \mathrm{d}p_\beta\,\mathrm{d}\nu(\mathbf{P})2\pi\delta(z - E_\beta)\langle\Psi_{nl},\mathbf{P}\,|\,\bar{\boldsymbol{\tau}}(z)\,|\,\beta\rangle\\ &\quad\times\langle\beta|\,\bar{\boldsymbol{\tau}}^\dagger(z)\,|\,\Psi_{nl},\mathbf{0}\rangle, \quad (5.17)\end{aligned}$$

and z is the solution of the master equation (3.10). Here, $\mathrm{d}p_\beta$ denotes the phase space integral over the intermediate state $|\beta\rangle$. At the accuracy we are considering, we may use $z = E_n$. In the following, we estimate the order of the various decays using this formula. As an illustration, we start with the decay into π^0K^0. The relative 3-momenta of the π^-K^+ pairs $\mathbf{p}$ and $\mathbf{p}'$ count as order δ and we have

$$\mathrm{d}\nu(\mathbf{p})\mathrm{d}\nu(\mathbf{p}')\Psi_{nl}^*(\mathbf{p})\Psi_{nl}(\mathbf{p}') = \mathcal{O}(\delta^3). \quad (5.18)$$

As can be read off from the energy delta function, the outgoing π^0 and K^0 3-momenta $\mathbf{p}_3$ and $\mathbf{p}_4$ count as order $\delta^{1/2}$. This leads to a phase space suppression factor of order $\delta^{1/2}$,

$$\mathrm{d}\nu(\mathbf{p}_3)\mathrm{d}\nu(\mathbf{p}_4)\delta^3(\mathbf{p}_3 + \mathbf{p}_4)\delta\left(E_n - E_{\pi^0K^0}\right) = \mathcal{O}(\delta^{1/2}), \quad (5.19)$$

where

$$E_{\pi^0K^0} = \Sigma_0 + \frac{\mathbf{p}_3^2}{2M_{\pi^0}} + \frac{\mathbf{p}_4^2}{2M_{K^0}}. \quad (5.20)$$

Further, the reduced matrix element ${}_+\langle\mathbf{p}\,|\,\bar{\boldsymbol{\tau}}(E_n)\,|\,\mathbf{p}_3\rangle_0$ is of $\mathcal{O}(1)$ and the S-wave decay width thus starts at order $\delta^{7/2}$. The relation (5.17) allows one to rather straightforwardly rederive the next-to-leading order formula for the decay width of the S-states. In order not to interrupt the argument, we relegate the relevant calculation to Appendix E, and continue here with the discussion of the radiative decay into $\pi^0K^0 + \gamma$. The outgoing π^0 and K^0 3-momenta again count as $\mathcal{O}(\delta^{1/2})$, while the outgoing photon 3-momentum $\mathbf{k}$ is of order δ. This can by seen by performing the phase space integrations over $\mathbf{p}_3$, $\mathbf{p}_4$ and $\mathbf{k}$ explicitly. In total, the phase space suppression factor amounts to $\delta^{5/2}$,

$$\begin{aligned}&\mathrm{d}\nu(\mathbf{p}_3)\mathrm{d}\nu(\mathbf{p}_4)\frac{\mathrm{d}^3\mathbf{k}}{2\,|\,\mathbf{k}|}\delta^3(\mathbf{p}_3 + \mathbf{p}_4 + \mathbf{k})\delta\left(E_n - E_{\pi^0K^0\gamma}\right)\\ &\quad = \mathcal{O}(\delta^{5/2}), \quad (5.21)\end{aligned}$$

with

$$E_{\pi^0K^0\gamma} = \Sigma_0 + \frac{\mathbf{p}_3^2}{2M_{\pi^0}} + \frac{\mathbf{p}_4^2}{2M_{K^0}} + |\,\mathbf{k}|\,. \quad (5.22)$$

The leading order contribution stems from Fig. 6a,b. The corresponding reduced matrix element is given by

$$\begin{aligned}&{}_+\langle\mathbf{p},-\mathbf{p}\,|\,\mathbf{V}\bar{\mathbf{G}}_{\rm C}^n\mathbf{V}\,|\,\mathbf{p}_3,\mathbf{p}_4,\mathbf{k},r\rangle_0\\ &= -eC_2\mathbf{p}\cdot\boldsymbol{\epsilon}(k,r) \quad (5.23)\\ &\quad\times\left[f(M_{\pi^+},\mathbf{p}^2,-\mathbf{p}\cdot\mathbf{k}) + f(M_{K^+},\mathbf{p}^2,\mathbf{p}\cdot\mathbf{k})\right] + \cdots,\end{aligned}$$

where

$$\begin{aligned}&f(M,\mathbf{p}^2,\pm\mathbf{p}\cdot\mathbf{k})\\ &\quad = \frac{1}{M}\left[\frac{\alpha^2\mu_+}{2n^2} + \frac{\mathbf{p}^2}{2\mu_+} + \frac{\mathbf{k}^2}{2M} + |\,\mathbf{k}|\,\pm\frac{\mathbf{p}\cdot\mathbf{k}}{M}\right]^{-1}. \quad (5.24)\end{aligned}$$

This matrix element is of order $\delta^{1/2}$ which implies that the decay width $\Gamma_{\pi^0K^0\gamma}$ starts at order $\delta^{13/2}$. However, this contribution vanishes after performing the integrations over $\mathbf{p}$ and $\mathbf{p}'$.

Next, we consider the decay into $K^0 + n\gamma$, $n = 1, 2$ (see Fig. 6c,d). Here, the outgoing K^0 and photon 3-momenta belong to the hard scale and thus count as $\mathcal{O}(1)$. For $\pi^-K^+ \to K^0 + \gamma$, the Lagrangian (5.14) leads to a reduced matrix element of order $\delta^{3/2}$,

$${}_+\langle\mathbf{p},-\mathbf{p}\,|\,\mathbf{V}\,|\,\mathbf{p}_4,\mathbf{k},r\rangle_0 = 2eD_1\mathbf{p}\cdot(\mathbf{k}\times\boldsymbol{\epsilon}(k,r)) + \cdots \quad (5.25)$$

Naive power counting implies that the decay width into $K^0 + \gamma$ starts at order δ^6. The matrix element (5.25) is

[5] Transitions between S-states with the simultaneous emission of two photons are not forbidden. However, they are suppressed by a factor of α^8.

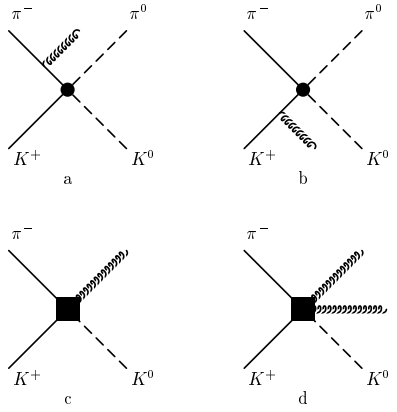

Fig. 6. Leading order contributions to the decays into $\pi^0 K^0 + \gamma$ and $K^0 + n\gamma$, $n = 1, 2$. The dot denotes the coupling C_2, while the box stands for the couplings D_1 and D_2 in $\mathcal{L}_{\rm A}$. The twisted lines denote transverse photons

odd in $\mathbf{p}$ and the S-wave decay width therefore even more suppressed, while $\Gamma_{n1,K^0\gamma}$ starts at order δ^6.

For the transition $\pi^- K^+ \to K^0 + 2\gamma$, we get from the Lagrangian (5.14) a local matrix element of order δ,

$$\begin{aligned} &{}_+(\mathbf{p}, -\mathbf{p} \mid \mathbf{V} \mid \mathbf{p}_4, \mathbf{k}_1, r_1, \mathbf{k}_2, r_2)_0 \\ &= e^2 D_2 k_1^0 \boldsymbol{\epsilon}(k_1, r_1) \cdot [\mathbf{k}_2 \times \boldsymbol{\epsilon}(k_2, r_2)] \\ &\quad -2e^2 D_1 \boldsymbol{\epsilon}(k_1, r_1) \cdot [\mathbf{k}_2 \times \boldsymbol{\epsilon}(k_2, r_2)] \\ &\quad + k_1 \leftrightarrow k_2, r_1 \leftrightarrow r_2, \end{aligned} \tag{5.26}$$

and the decay width of the S-states into $K^0 + 2\gamma$ thus starts at order δ^5. For the P-wave decay width into $K^0 + 2\gamma$ this contributions vanishes, because the matrix element in (5.26) is $\mathbf{p}$ independent.

Processes with a higher number of photons may be treated in an analogous manner. We expect them – using power counting arguments – to be even more suppressed. Since hard processes such as $K^0 + n_1\gamma + n_2 e^+ e^-$, $n_1 + n_2 > 0$ do not contribute to the decay width at order $\delta^{9/2}$, we may assume that all couplings in the non-relativistic Lagrangian in (A.2), (A.4) and (A.5) are real. The total S-wave decay width of the $\pi^- K^+$ atom amounts to

$$\Gamma_{n0} = \Gamma_{n0,\pi_0 K_0} + \mathcal{O}(\delta^5). \tag{5.27}$$

The $\pi^- K^+$ atom in the 2P-state on the other hand decays predominantly through the radiative transition into the ground state. To evaluate this transition, we insert the ground state plus one photon into (5.17). Here the photon 3-momentum $\mathbf{k}$ counts as order δ^2, as can be read off from the energy delta function $\delta(E_2 - E_1 - |\mathbf{k}|)$. At leading order, we get for the spontaneous $2p$–$1s$ transition the well-known expression, see e.g. [57]

$$\Gamma_{21} = \left(\frac{2}{3}\right)^8 \alpha^5 \mu_+ + \cdots \tag{5.28}$$

The result is of order α^5 and given numerically in Table 3. The first subleading decay mode of the 2P-state starts at order δ^6 with the odd intrinsic parity decay into $K^0 + \gamma$. The P-wave decay width into $\pi^0 K^0$ in (4.6) is of order $\delta^{13/2}$ and suppressed with respect to the radiative $2p$–$1s$ transition by a factor of 10^{-7}.

6 Vacuum polarization

What remains to be added are the contributions coming from the electron vacuum polarization. The calculation of these corrections within a non-relativistic Lagrangian approach has been performed in [22]. In our framework, the contributions due to vacuum polarization arise formally at higher order in α. However, they are amplified by powers of the coefficient μ_+/m_e, where m_e denotes the electron mass. To the accuracy considered here, the only effect of the vacuum polarization of the electron is a modification of the Coulomb potential $\mathbf{H}_{\rm C} \to \mathbf{H}_{\rm C} + \mathbf{H}_{\rm vac}$, with

$$\begin{aligned} {}_+(\mathbf{p} \mid \mathbf{H}_{\rm vac} \mid \mathbf{q})_+ &= -\frac{4\alpha^2}{3} \int_{4m_e^2}^{\infty} \frac{{\rm d}s}{s + (\mathbf{p}-\mathbf{q})^2} \frac{1}{s} \\ &\quad \times \left[1 + \frac{2m_e^2}{s}\right] \left[1 - \frac{4m_e^2}{s}\right]^{1/2}. \end{aligned} \tag{6.1}$$

The vacuum polarization leads to an electromagnetic energy shift evaluated in [22,25,44],

$$\Delta E_{nl}^{\rm vac} = (\Psi_{nl} \mid \mathbf{H}_{\rm vac} \mid \Psi_{nl}). \tag{6.2}$$

For the first two energy-level shifts of pionium[6] and the $\pi^\pm K^\mp$ atom, $\Delta E_{\pi,nl}^{\rm vac}$ and $\Delta E_{nl}^{\rm vac}$ are given numerically in Tables 2 and 3. Formally of order α^{2l+5}, this contribution is numerically sizable due to its large coefficient containing $(\mu_+/m_e)^{2l+2}$.

The vacuum polarization also interferes with strong interactions and contributes to the decay width and to the strong energy shift. This can be seen by inserting the modified Coulomb potential into the master equation (3.10). For the spectrum and the width of the $\pi^\pm K^\mp$ atom, we get

$$\begin{aligned} \Gamma_{n0} &= \frac{8\alpha^3 \mu_+^2}{n^3} p_n^* (a_0^-)^2 \left(1 + \delta_{K,n} + \delta_{K,n}^{\rm vac}\right), \\ \Delta E_{n0}^{\rm h} &= -\frac{2\alpha^3 \mu_+^2}{n^3} (a_0^+ + a_0^-) \left(1 + \delta'_{K,n} + \delta_{K,n}^{\rm vac}\right). \end{aligned} \tag{6.3}$$

What concerns pionium, the decay width and strong energy shift are modified, according to

$$\begin{aligned} \Gamma_{\pi,n0} &= \frac{2\alpha^3}{9n^3} p_{\pi,n}^* (a_0^0 - a_0^2)^2 \left(1 + \delta_{\pi,n} + \delta_{\pi,n}^{\rm vac}\right), \\ \Delta E_{\pi,n0}^{\rm h} &= -\frac{\alpha^3 M_{\pi^+}}{6n^3} (2a_0^0 + a_0^2) \left(1 + \delta'_{\pi,n} + \delta_{\pi,n}^{\rm vac}\right). \end{aligned} \tag{6.4}$$

The correction $\delta_{h,n}^{\rm vac}$, $h = \pi, K$ is proportional to the change in the Coulomb wave function [22] of the bound system due to vacuum polarization,

$$\delta_{h,n}^{\rm vac} = \frac{2\delta\Psi_{n0}(\mathbf{x}=0)}{\Psi_{n0}(\mathbf{x}=0)}. \tag{6.5}$$

[6] For pionium, the electromagnetic energy shift due to vacuum polarization is denoted by $\Delta E_{\pi,nl}^{\rm vac}$.

Table 2. Numerical values for the energy shift and the lifetime of the $\pi^+\pi^-$ atom

$\pi^+\pi^-$ atom	$\Delta E^{\rm em}_{\pi,nl}$ [eV]	$\Delta E^{\rm vac}_{\pi,nl}$ [eV]	$\Delta E^{\rm h}_{\pi,nl}$ [eV]	$10^{15}\tau_{\pi,nl}$[s]
$n=1,\, l=0$	-0.065	-0.942	-3.8 ± 0.1	2.9 ± 0.1
$n=2,\, l=0$	-0.012	-0.111	-0.47 ± 0.01	23.3 ± 0.7
$n=2,\, l=1$	-0.004	-0.004	$\simeq -1 \cdot 10^{-6}$	$\simeq 1.2 \cdot 10^4$

Table 3. Numerical values for the energy shift and the lifetime of the $\pi^\pm K^\mp$ atom

$\pi^\pm K^\mp$ atom	$\Delta E^{\rm em}_{nl}$ [eV]	$\Delta E^{\rm vac}_{nl}$ [eV]	$\Delta E^{\rm h}_{nl}$ [eV]	$10^{15}\tau_{nl}$[s]
$n=1,\, l=0$	-0.095	-2.56	-9.0 ± 1.1	3.7 ± 0.4
$n=2,\, l=0$	-0.019	-0.29	-1.1 ± 0.1	29.4 ± 3.3
$n=2,\, l=1$	-0.006	-0.02	$\simeq -3 \cdot 10^{-6}$	$\simeq 0.7 \cdot 10^4$

Here, Ψ_{nl} stands for a generic Coulomb wave function and $h = \pi, K$. For the ground state, this result is contained in Table II of [22]. Formally, $\delta^{\rm vac}_{h,n}$ is of order α^2, but enhanced because of the large coefficient containing μ_+/m_e.

7 Numerics

In the numerical evaluation of the widths and energy shifts of the $\pi^+\pi^-$ and $\pi^\pm K^\mp$ atoms, we use the following numbers: The $\pi\pi$ scattering lengths yield $a_0^0 = 0.220 \pm 0.005$, $a_0^2 = -0.0444 \pm 0.0010$ and $a_1^1 = (0.379 \pm 0.005) \cdot 10^{-1} M_{\pi^+}^{-2}$ [4,5]. The correlation matrix for a_0^0 and a_0^2 is given in [5]. For the isospin symmetry breaking corrections to the $\pi\pi$ threshold amplitudes (4.14) and (4.17) at order e^2p^2, we use $\epsilon_\pi = (0.61 \pm 0.16) \cdot 10^{-2}$ and $\epsilon'_\pi = (0.37 \pm 0.08) \cdot 10^{-2}$ [23,54]. The values for the πK scattering lengths are taken from the recent analysis of data and Roy–Steiner equations [33]. The S-wave scattering lengths yield $a_0^+ = (0.045 \pm 0.012) M_{\pi^+}^{-1}$, $a_0^- = (0.090 \pm 0.005) M_{\pi^+}^{-1}$ [33], and for the P-waves we use $a_1^{1/2} = (0.19 \pm 0.01) \cdot 10^{-1} M_{\pi^+}^{-3}$ and $a_1^{3/2} = (0.65 \pm 0.44) \cdot 10^{-3} M_{\pi^+}^{-3}$ [33]. The correlation parameter for a_0^+ and a_0^- is also given in [33]. The isospin breaking corrections to the πK threshold amplitudes (4.4) and (4.9) have been worked out in [36,50,51] at $\mathcal{O}(p^4, e^2p^2)$. Whereas the analytic expressions for ϵ and ϵ' obtained in [36,50,51] are not identical, the numerical values agree within the uncertainties quoted in [51]. In the following, we use [51] $\epsilon = (0.1 \pm 0.1) \cdot 10^{-2} M_{\pi^+}^{-1}$ and $\epsilon' = (0.1 \pm 0.3) \cdot 10^{-2} M_{\pi^+}^{-1}$. For the charge radii of the pion and kaon, we take $\langle r^2_{\pi^+} \rangle = (0.452 \pm 0.013)\,\mathrm{fm}^2$ and $\langle r^2_{K^+} \rangle = (0.363 \pm 0.072)\,\mathrm{fm}^2$ [58]. In the evaluation of the uncertainties, we take into account the correlation between the $\pi\pi$ (πK) scattering lengths.

The isospin breaking corrections $\delta_{h,n}$ and $\delta'_{h,n}$, $h = \pi, K$ to the widths (4.5) and (4.16) and strong energy shifts (4.10) and (4.18) are listed in Table 1. The energy shift corrections $\delta'_{K,n}$ are smaller than in the case of pionium. This distinction comes from the different size of the isospin breaking contributions to the elastic one-particle irreducible $\pi\pi$ and πK amplitudes. At leading order in the chiral expansion, the isospin breaking part of the $\pi^-K^+ \to \pi^-K^+$ amplitude at threshold is suppressed by a factor of M_{π^+}/M_{K^+} with respect to the corresponding quantity in $\pi\pi$ scattering.

As described in Sect. 6, (6.3) and (6.4), the width and strong energy shift are modified due to vacuum polarization, according to

$$\delta_{h,n} \to \delta_{h,n} + \delta^{\rm vac}_{h,n}, \quad \delta'_{h,n} \to \delta'_{h,n} + \delta^{\rm vac}_{h,n}, \tag{7.1}$$

where $h = \pi, K$ and $\delta^{\rm vac}_{h,n}$ is defined in (6.5). For the ground state, the corrections due to vacuum polarization yield $\delta^{\rm vac}_{K,1} = 0.45 \cdot 10^{-2}$ and $\delta^{\rm vac}_{\pi,1} = 0.31 \cdot 10^{-2}$ [22]. However, for the numerical analysis of the width and the strong energy shift, we may neglect the contributions from $\delta^{\rm vac}_{h,n}$, because the uncertainties in $\delta_{h,n}$ and $\delta'_{h,n}$ are larger than $\delta^{\rm vac}_{h,n}$ itself.

For the first two states of the $\pi^+\pi^-$ and $\pi^\pm K^\mp$ atoms, the numerical values for the lifetime $\tau_{nl} \doteq \Gamma_{nl}^{-1}$, ($\tau_{\pi,nl} \doteq \Gamma_{\pi,nl}^{-1}$) and the energy shifts are listed in Tables 2 and 3. The numbers for the lifetime and strong energy shifts of the S-states are valid at next-to-leading order in isospin symmetry breaking. The bulk part in the uncertainties of these quantities is due to the uncertainties in the corresponding scattering lengths. For the lifetime of the 2P-state, the numerical values are valid at leading order only, and determined by the $2p$–$1s$ radiative transition in (5.28) [59].

The energy-level shift due to vacuum polarization $\Delta E^{\rm vac}_{nl}$ ($\Delta E^{\rm vac}_{\pi,nl}$) [22,44] is specified in (6.2). Formally of higher order in α, this contribution is numerically sizable. We do not display the error bars for the electromagnetic energy shifts. At order α^4, they come from the uncertainties in the charge radii of the pion and kaon only. In the case of pionium, the uncertainties of $\Delta E^{\rm em}_{\pi,10}$ at order α^4 amount to about 0.7%, while for the $\pi^\pm K^\mp$ atom $\Delta E^{\rm em}_{10}$ is known at the 5% level. To estimate the order of magnitude of the electromagnetic corrections at higher order, we may compare with positronium. Here, the α^5 and $\alpha^5 \ln\alpha$ corrections [60] amount to about 2% with respect to the α^4 contributions.

Both, the electromagnetic and vacuum polarization contributions to the energy shift are known to a high

accuracy. A future precision measurement of the energy splitting between the nS and nP states [61] will therefore allow one to extract the strong S-wave energy shift in (4.10), and to determine the combination $a_0^+ + a_0^-$ of the πK scattering lengths. The $2s$–$2p$ energy splitting yields

$$\begin{aligned}\Delta E_{2s-2p} &= \Delta E_{20}^{\rm h} + \Delta E_{20}^{\rm em} - \Delta E_{21}^{\rm em} + \Delta E_{20}^{\rm vac} - \Delta E_{21}^{\rm vac} \\ &= -1.4 \pm 0.1\,{\rm eV}. \end{aligned} \tag{7.2}$$

The uncertainty displayed is the one in $\Delta E_2^{\rm h}$ only. To the accuracy we are working, we may neglect the strong shift in the 2P state; it is suppressed by the power of α^5. For pionium the energy splitting between the 2S and 2P states reads

$$\begin{aligned}&\Delta E_{\pi,2s-2p} \\ &= \Delta E_{\pi,20}^{\rm h} + \Delta E_{\pi,20}^{\rm em} - \Delta E_{\pi,21}^{\rm em} + \Delta E_{\pi,20}^{\rm vac} - \Delta E_{\pi,21}^{\rm vac} \\ &= -0.59 \pm 0.01\,{\rm eV}. \end{aligned} \tag{7.3}$$

Again the uncertainty displayed is the one in $\Delta E_{\pi,2}^{\rm h}$ only and we may neglect contributions from the strong shift in the 2P state.

As an illustration, we alternatively use the ChPT predictions for the πK scattering lengths [34,36] in the numerical evaluation of the lifetime. The ChPT predictions yield at order p^4, $a_0^+ = (0.032 \pm 0.016) M_{\pi^+}^{-1}$ and $a_0^- = (0.079 \pm 0.001) M_{\pi^+}^{-1}$ [33]. Here, the errors include the uncertainties in the values of the input parameters only. The uncertainty in a_0^- is remarkably small, because the isospin odd scattering length involves at $\mathcal{O}(p^4)$ a single low-energy constant $L_5^{\rm r}$ [36]. On the other hand, a_0^+ contains apart from the combination $2L_6^{\rm r} + L_8^{\rm r}$ five further coupling constants [36], which are enhanced by one power of M_{K^+}/M_{π^+} with respect to the counterterm in a_0^-. For a_0^-, the two-loop correction has to be rather substantial, in order to reproduce the central value of the Roy–Steiner evaluation. Very recently, the chiral expansion of the πK scattering amplitude at next-to-next-to-leading order became available [37]. According to the preliminary numerical study performed in [37], the S-wave scattering lengths are at order p^6 in reasonable agreement with the Roy–Steiner evaluation [33]. The $\mathcal{O}(p^4)$ ChPT prediction for the lifetime of the $\pi^\pm K^\mp$ atom in its ground state is

$$\tau_{10} = 4.7 \cdot 10^{-15}\,{\rm s}, \quad {\rm ChPT}[\mathcal{O}(p^4)], \tag{7.4}$$

whereas

$$\tau_{10} = (3.7 \pm 0.4) \cdot 10^{-15}\,{\rm s}, \quad \text{Roy–Steiner}. \tag{7.5}$$

The ChPT prediction is valid at next-to-leading order in isospin symmetry breaking and up to and including $\mathcal{O}(p^4)$ in the chiral expansion.

8 Summary and outlook

We have considered the spectra and decays of $\pi^+\pi^-$ and $\pi^\pm K^\mp$ atoms in the framework of QCD + QED. We evaluated the corrections to the Deser-type formulae for the width and the energy shift – valid at next-to-leading order in isospin symmetry breaking – within a non-relativistic effective field theory. It is convenient to introduce a different book keeping for the $\pi^+\pi^-$ and $\pi^\pm K^\mp$ atoms. As concerns pionium, we count α and $(m_u - m_d)^2$ as small quantities of order δ; in the case of the $\pi^\pm K^\mp$ atom both α and $m_u - m_d$ are of order δ. The different counting schemes are due to the fact that in QCD, the pion mass difference starts at $(m_u - m_d)^2$, while the kaon mass difference is linear in $m_u - m_d$.

Consider first the energy shifts that are split into an electromagnetic and a strong part, according to (2.1). The electromagnetic part in (5.12) and (5.13) contains both pure QED contributions as well as finite size effects due to the charge radii of the pion and kaon. The strong energy shift of the $\pi^- K^+$ atom is proportional to the one-particle irreducible $\pi^- K^+ \to \pi^- K^+$ scattering amplitude at threshold. In the isospin symmetry limit, the elastic threshold amplitude reduces to the sum of isospin even and odd scattering lengths $a_0^+ + a_0^-$. The isospin breaking contributions to the amplitude have been evaluated at $\mathcal{O}(e^2 p^2, p^4)$ [36,51] in the framework of ChPT. The result in (4.10) displays the S-wave energy shift in terms of the sum $a_0^+ + a_0^-$ and a correction of order α and $m_u - m_d$. For the first two energy-level shifts, the isospin symmetry breaking correction modifies the leading order term at the 2% level. The isospin even scattering length a_0^+ is sensitive to the combination of low-energy constants $2L_6^{\rm r} + L_8^{\rm r}$. The consequences of this observation for the SU(3)×SU(3) quark condensate [39] remain to be worked out. In the case of pionium, the strong energy shift displayed in (4.18) is related to the $\pi\pi$ scattering lengths combination $2a_0^0 + a_0^2$ and a correction of order α and $(m_u - m_d)^2$. For the first two energy levels, these isospin symmetry breaking contributions amount to about 6%.

A future measurement of the energy splitting between the 2S and 2P state in the $\pi^+\pi^-$ ($\pi^\pm K^\mp$) atom will allow one to extract the strong energy shift and to determine the scattering lengths combination $2a_0^0 + a_0^2$ ($a_0^+ + a_0^-$). This is due to the fact that the electromagnetic energy shifts are known to high accuracy and the strong P-wave energy shifts in (4.12) and (4.19) are suppressed by the power of α^5. However, another higher order correction – generated by the vacuum polarization – is numerically sizable and contributes to the energy splitting in (7.2) and (7.3). Formally of order α^{2l+5}, this correction is enhanced due to its large coefficient containing $(\mu_+/m_e)^{2l+2}$.

We now turn to the decay widths of the $\pi^+\pi^-$ and $\pi^- K^+$ atoms. At leading and next-to-leading order the $\pi^+\pi^-$ and $\pi^- K^+$ atoms decay into $2\pi^0$ and $\pi^0 K^0$ exclusively. Aside from a kinematical factor – the relativistic outgoing 3-momentum of the bound system – their decay width can be expanded in powers of α and $m_u - m_d$. By invoking ChPT, the result for the S-wave decay width of the $\pi^- K^+$ atom may be expressed in terms of the isospin odd scattering length a_0^-, and an isospin symmetry breaking correction of order α and $m_u - m_d$; see (4.5). For the ground-state decay width, this correction modifies the leading order Deser-type relation at the 4% level. The

next-to-leading order result for the S-wave decay width of pionium is given in (4.16). The expression for the ground-state width agrees with the result obtained in [20,23,30].

For the 2P state of the $\pi^- K^+$ ($\pi^+\pi^-$) atom, the decay width starts at order α^5 with the $2p$–$1s$ radiative transition into the ground state; see (5.28). The P-wave decay width of the $\pi^- K^+$ atom into $\pi^0 K^0$ in (4.6) is suppressed by the power of $\delta^{13/2}$. For pionium, the P-wave decay width into a pair of two neutral pions vanishes due to C invariance.

We find it very exciting that in view of the beautiful work performed by our experimental colleagues, we may expect that many of the above predictions will be confronted with experimental data in a not too distant future. This will certainly improve our knowledge of the low-energy structure of QCD.

Acknowledgements. I am grateful to J. Gasser for his help and advice throughout this work and for reading the manuscript carefully. I thank P. Büttiker, R. Kaiser, B. Kubis, A. Rusetsky, H. Sazdjian and J. Schacher for useful discussions. This work was supported in part by the Swiss National Science Foundation and by RTN, BBW-Contract N0. 01.0357 and EC-Contract HPRN–CT2002–00311 (EURIDICE).

A Non-relativistic Lagrangian

The non-relativistic Lagrangian must be invariant under space rotation, P, T and gauge transformations. We do not include terms corresponding to transitions between sectors with different numbers of heavy fields (pions and kaons). These interactions describe processes with an energy release at the hard scale. In general, such decay processes are accounted for by introducing complex couplings in the non-relativistic Lagrangian. However, as shown in Sect. 5.2, intermediate states do not contribute to the decay width at order $\delta^{9/2}$ and we may therefore assume the low-energy couplings to be real.

In the sector with one or two mesons, the non-relativistic effective Lagrangian is given by

$$\mathcal{L}_{\rm NR} = \mathcal{L}_1 + \mathcal{L}_2^{(0)} + \mathcal{L}_2^{(2)} + \cdots \tag{A.1}$$

The first term contains the one-pion and one-kaon sectors:

$$\begin{aligned}
\mathcal{L}_1 = {}& \frac{1}{2}(\mathbf{E}^2 - \mathbf{B}^2) \\
& + \pi_0^\dagger \left(\mathrm{i}\partial_t - M_{\pi^0} + \frac{\Delta}{2M_{\pi^0}} + \frac{\Delta^2}{8M_{\pi^0}^3} + \cdots \right) \pi_0 \\
& + K_0^\dagger \left(\mathrm{i}\partial_t - M_{K^0} + \frac{\Delta}{2M_{K^0}} + \frac{\Delta^2}{8M_{K^0}^3} + \cdots \right) K_0 \\
& + \sum_\pm \pi_\pm^\dagger \left(\mathrm{i}D_t - M_{\pi^+} + \frac{\mathbf{D}^2}{2M_{\pi^+}} + \frac{\mathbf{D}^4}{8M_{\pi^+}^3} + \cdots \right) \pi_\pm \\
& + \sum_\pm K_\pm^\dagger \left(\mathrm{i}D_t - M_{K^+} + \frac{\mathbf{D}^2}{2M_{K^+}} + \frac{\mathbf{D}^4}{8M_{K^+}^3} + \cdots \right) K_\pm \\
& \mp e \sum_\pm \mathbf{D}(\mathbf{E}) \left(\frac{c_\pi}{6M_{\pi^+}^2} \pi_\pm^\dagger \pi_\pm + \frac{c_K}{6M_{K^+}^2} K_\pm^\dagger K_\pm + \cdots \right),
\end{aligned} \tag{A.2}$$

with electromagnetic charge e, $\mathbf{E} = -\nabla A_0 - \dot{\mathbf{A}}$ and $\mathbf{B} = \nabla \times \mathbf{A}$. The covariant derivatives of the charged meson fields are given by

$$\begin{aligned}
D_t \pi_\pm &= \partial_t \pi_\pm \mp \mathrm{i}eA_0 \pi_\pm, \quad \mathbf{D}\pi_\pm = \nabla\pi_\pm \pm \mathrm{i}e\mathbf{A}\pi_\pm, \\
D_t K_\pm &= \partial_t K_\pm \mp \mathrm{i}eA_0 K_\pm, \quad \mathbf{D}K_\pm = \nabla K_\pm \pm \mathrm{i}e\mathbf{A}K_\pm.
\end{aligned} \tag{A.3}$$

The one-pion–one-kaon sector of total zero charge reads at lowest order

$$\begin{aligned}
\mathcal{L}_2^{(0)} = {}& C_1 \pi_-^\dagger K_+^\dagger \pi_- K_+ + C_2 \left(\pi_-^\dagger K_+^\dagger \pi_0 K_0 + \text{h.c.} \right) \\
& + C_3 \pi_0^\dagger K_0^\dagger \pi_0 K_0.
\end{aligned} \tag{A.4}$$

To evaluate the decay width and energy shifts of the $\pi^- K^+$ atom, we need in addition the following terms with two covariant space derivatives[7]:

$$\begin{aligned}
\mathcal{L}_2^{(2)} = {}& C_4 \left(\pi_-^\dagger \overleftrightarrow{\mathbf{D}}^2 K_+^\dagger \pi_0 K_0 + \text{h.c.} \right) \\
& + C_5 \left(\pi_-^\dagger \overleftrightarrow{\mathbf{D}}^2 K_+^\dagger \pi_- K_+ + \text{h.c.} \right) \\
& + C_6 (\pi_-^\dagger \pi_-) \mathbf{D}^2 (K_+^\dagger K_+) \\
& + C_7 \left(\nabla \pi_-^\dagger K_+^\dagger \nabla \pi_0 K_0 + \text{h.c.} \right) + \cdots,
\end{aligned} \tag{A.5}$$

where $u \overleftrightarrow{\mathbf{D}}^2 v \doteq u\mathbf{D}^2 v + v\mathbf{D}^2 u$. We work in the center of mass system and thus omit terms proportional to the CM momentum. We do not display time derivatives, for on-shell matrix elements they can be eliminated by the use of the equations of motion. The parameters M_{π^i} (M_{K^i}) denote the physical pion, (kaon) masses – there is no mass renormalization in the non-relativistic theory; see Sect. 3.3.

We work in the Coulomb gauge and eliminate the A^0 component of the photon field by the use of the equations of motion. At the accuracy we are considering, the term linear in $\mathbf{D}(\mathbf{E})$ in (A.2) then reduces to a local interaction which modifies the low-energy coupling C_1,

$$\begin{aligned}
C_1' &= C_1 - e^2\lambda, \\
\lambda &= \frac{c_\pi}{6M_{\pi^+}^2} + \frac{c_K}{6M_{K^+}^2}.
\end{aligned} \tag{A.6}$$

It is sufficient to match the non-relativistic couplings c_π and c_K at order δ^0. We therefore consider the pion and

[7] In the CM system and by the use of the equations of motion, we identify

$$\begin{aligned}
\pi_-^\dagger K_+^\dagger \pi_0 \overleftrightarrow{\Delta} K_0 = {}& -4\mu_0(\Sigma_+ - \Sigma_0) \pi_-^\dagger K_+^\dagger \pi_0 K_0 \\
& + \frac{\mu_0}{\mu_+} \pi_-^\dagger \overleftrightarrow{\mathbf{D}}^2 K_+^\dagger \pi_0 K_0.
\end{aligned}$$

kaon electromagnetic form-factors in the external field A_μ. The results of the matching yield

$$c_\pi = M_{\pi^+}^2 \langle r_\pi^2 \rangle, \quad c_K = M_{K^+}^2 \langle r_K^2 \rangle, \tag{A.7}$$

where r_π and r_K denote the charge radii of the charged pion and kaon, respectively. The remaining low-energy constants C_i, $i = 1, \ldots, 7$ may be determined through matching the πK amplitude in the vicinity of the threshold for different channels; see Sect. 3.3.

B Relativistic scattering amplitudes

First, we consider the $S = 1$ processes

$$\pi^- K^+ \to \pi^- K^+, \quad \pi^- K^+ \to \pi^0 K^0, \quad \pi^0 K^0 \to \pi^0 K^0, \tag{B.1}$$

in the isospin symmetry limit. The decomposition into amplitudes with definite isospin yields

$$\begin{aligned} T^{\pm;\pm} &= \frac{1}{3}\left[T^{3/2}(s,t) + 2T^{1/2}(s,t)\right], \\ T^{00;\pm} &= \frac{\sqrt{2}}{3}\left[T^{3/2}(s,t) - T^{1/2}(s,t)\right], \\ T^{00;00} &= \frac{1}{3}\left[2T^{3/2}(s,t) + T^{1/2}(s,t)\right]. \end{aligned} \tag{B.2}$$

The isospin $I = 1/2$ and $I = 3/2$ components are related via

$$T^{1/2}(s,t,u) = \frac{3}{2}T^{3/2}(u,t,s) - \frac{1}{2}T^{3/2}(s,t,u). \tag{B.3}$$

The T^+ (T^-) amplitude

$$\begin{aligned} T^+(s,t) &= \frac{1}{3}\left[T^{1/2}(s,t) + 2T^{3/2}(s,t)\right], \\ T^-(s,t) &= \frac{1}{3}\left[T^{1/2}(s,t) - T^{3/2}(s,t)\right], \end{aligned} \tag{B.4}$$

is even (odd) under $s \leftrightarrow u$ crossing. In the s-channel, the decomposition into partial waves reads

$$T^I(s,t) = 16\pi \sum_{l=0}^{\infty} (2l+1) t_l^I(s) P_l(\cos\theta), \tag{B.5}$$

where $s = [\omega_{\pi^+}(\mathbf{p}) + \omega_{K^+}(\mathbf{p})]^2$, $t = -2\mathbf{p}^2(1-\cos\theta)$ and θ is the scattering angle in the CM system.

The real part of the partial wave amplitudes near threshold is of the form,

$$\mathrm{Re}\, t_l^I(s) = \frac{\sqrt{s}}{2}\mathbf{p}^{2l}\left(a_l^I + b_l^I \mathbf{p}^2 + \mathcal{O}(\mathbf{p}^4)\right), \tag{B.6}$$

where a_l^I denote the scattering lengths and b_l^I the effective ranges.

There follow the $\pi\pi$ scattering processes:

$$\pi^-\pi^+ \to \pi^-\pi^+, \quad \pi^-\pi^+ \to \pi^0\pi^0, \tag{B.7}$$

with

$$\begin{aligned} T_\pi^{\pm;\pm} &= \frac{1}{6}\left[T_\pi^2(s,t) + 3T_\pi^1(s,t) + 2T_\pi^0(s,t)\right], \\ T_\pi^{00;\pm} &= \frac{1}{3}\left[T_\pi^2(s,t) - T_\pi^0(s,t)\right]. \end{aligned} \tag{B.8}$$

The decomposition into partial waves yields

$$T_\pi^I(s,t) = 32\pi \sum_{l=0}^{\infty} (2l+1) P_l(\cos\theta) t_{\pi,l}^I(s), \tag{B.9}$$

where $s = 4(M_{\pi^+}^2 + \mathbf{p}^2)$. At threshold, the partial wave amplitudes take the form

$$\mathrm{Re} t_{\pi,l}^I(s) = \mathbf{p}^{2l}\left[a_l^I + \mathbf{p}^2 b_l^I + \mathcal{O}(\mathbf{p}^4)\right]. \tag{B.10}$$

C Schwinger's Green function

The Schwinger Green function fulfills

$$\begin{aligned} &\left[E - \frac{\mathbf{q}^2}{2\mu_+}\right] {}_+\langle \mathbf{q}|\, \mathbf{G}_\mathrm{C}(z)\, |\mathbf{p}\rangle_+ \\ &+ e^2 \int \mathrm{d}\nu(k) \frac{1}{(\mathbf{k}-\mathbf{q})^2} {}_+\langle \mathbf{k}|\, \mathbf{G}_\mathrm{C}(z)\, |\mathbf{p}\rangle_+ \\ &= (2\pi)^3 \delta^3(\mathbf{q}-\mathbf{p}), \end{aligned} \tag{C.1}$$

where $E = z - \Sigma_+$. The explicit expression is given by[8]

$$\begin{aligned} &{}_+\langle \mathbf{q}|\, \mathbf{G}_\mathrm{C}(z)\, |\mathbf{p}\rangle_+ \\ &= \frac{(2\pi)^3\delta^3(\mathbf{q}-\mathbf{p})}{E - \frac{\mathbf{q}^2}{2\mu_+}} - \frac{1}{E - \frac{\mathbf{q}^2}{2\mu_+}} \frac{4\pi\alpha}{(\mathbf{q}-\mathbf{p})^2} \frac{1}{E - \frac{\mathbf{p}^2}{2\mu_+}} \\ &\quad - \frac{1}{E - \frac{\mathbf{q}^2}{2\mu_+}} 4\pi\alpha\eta I(E,\mathbf{q},\mathbf{p}) \frac{1}{E - \frac{\mathbf{p}^2}{2\mu_+}}, \end{aligned} \tag{C.2}$$

with $\eta = \alpha/2(-E/(2\mu_+))^{-1/2}$. The function

$$\begin{aligned} I(E,\mathbf{q},\mathbf{p}) = \int_0^1 \mathrm{d}\rho \rho^{-\eta} \Bigg[&(\mathbf{q}-\mathbf{p})^2\rho + \frac{\eta^2}{\alpha^2}(1-\rho^2) \\ &\times \left(E - \frac{\mathbf{q}^2}{2\mu_+}\right)\left(E - \frac{\mathbf{p}^2}{2\mu_+}\right)\Bigg]^{-1}, \end{aligned} \tag{C.3}$$

contains poles at $\eta = 1, 2, \ldots$ or, equivalently, at $z = E_n$. The integral

$$\begin{aligned} \langle \bar{\mathbf{g}}_\mathrm{C}^n(E_n) \rangle &= \int \frac{\mathrm{d}^d\mathbf{p}}{(2\pi)^d} \frac{\mathrm{d}^d\mathbf{q}}{(2\pi)^d} {}_+\langle \mathbf{q}|\, \bar{\mathbf{G}}_\mathrm{C}^n(E_n)\, |\mathbf{p}\rangle_+ \\ &= \frac{\alpha\mu_+^2}{\pi}\left\{\psi(n) - \psi(1) - \frac{1}{n} \right. \\ &\quad \left. + \frac{1}{2}\left[\Lambda(\mu) - 1 + 2\ln\frac{\alpha}{n} + \ln\frac{4\mu_+^2}{\mu^2}\right]\right\}, \end{aligned} \tag{C.4}$$

with $\psi(n) = \Gamma'(n)/\Gamma(n)$ develops an ultraviolet singularity as $d \to 3$,

$$\Lambda(\mu) = (\mu^2)^{d-3}\left\{\frac{1}{d-3} - \Gamma'(1) - \ln 4\pi\right\}. \tag{C.5}$$

[8] To simplify the notation, we omit the positive imaginary part in E.

D Non-relativistic integrals

What follows is a list of the non-relativistic integrals used to calculate the πK scattering amplitudes in Sect. 3.3 as well as in the evaluation of the decay width (Sect. 3.2) and energy shifts (Sects. 3.2 and 5.1). Whenever necessary, the integrations are worked out in $D \neq 4$ space-time dimensions to take care of possible ultraviolet or infrared divergences.

The non-relativistic propagator of the heavy fields reads

$$\begin{aligned} G_{\mathrm{NR},h}(x) &\doteq \mathrm{i}\langle 0|T\bar{h}(x)\bar{h}^\dagger(0)|0\rangle \\ &= \int \frac{\mathrm{d}^D p}{(2\pi)^D} \mathrm{e}^{-\mathrm{i}px} \frac{1}{M_h + \frac{\mathbf{p}^2}{2M_h} - p^0 - \mathrm{i}\epsilon}, \end{aligned} \tag{D.1}$$

where $\bar{h}$ stands for the free fields, with $h = \pi^-, \pi^0, K^+, K^0$ and M_h denotes the corresponding mass. The tadpole diagram $G_{\mathrm{NR},h}(0)$ vanishes in dimensional regularization. This can be seen by performing the integration over the zero-component of the loop momentum explicitly. The remaining integral is scaleless and therefore zero in dimensional regularization.

At $\alpha = 0$, the elementary loop function to calculate a diagram with any number of bubbles is given by

$$\begin{aligned} &J_i(P^0) \\ &= \frac{1}{\mathrm{i}} \int \frac{\mathrm{d}^D l}{(2\pi)^D} \frac{1}{M_{\pi^i} + \frac{\mathbf{l}^2}{2M_{\pi^i}} - l^0} \frac{1}{M_{K^i} + \frac{\mathbf{l}^2}{2M_{K^i}} - P^0 + l^0}, \end{aligned} \tag{D.2}$$

where $i = +, 0$. After the integration over the zero-component of the loop momentum, we arrive at

$$J_i(P^0) = \int \frac{\mathrm{d}^d \mathbf{l}}{(2\pi)^d} \frac{1}{\Sigma_i + \frac{\mathbf{l}^2}{2\mu_i} - P^0}. \tag{D.3}$$

The function is analytic in the complex P^0 plane, except for a cut on the real axis for $P^0 \geq \Sigma_i$. For $P^0 \geq \Sigma_i$ and $d \neq 3$, we get

$$\begin{aligned} J_i(P^0) = \frac{\mathrm{i}\mu_i^{3/2}}{\sqrt{2}\pi} \sqrt{P^0 - \Sigma_i} \Bigg[1 + \frac{d-3}{2} \\ \times \left(-\mathrm{i}\pi - 2 - \Gamma'(1) + \ln 4\pi + \ln 2\mu_i (P^0 - \Sigma_i) \right) \Bigg]. \end{aligned} \tag{D.4}$$

To obtain the contribution to the scattering amplitude, we need to evaluate this function at $P^0 = \omega_{\pi^+}(\mathbf{p}) + \omega_{K^+}(\mathbf{p})$. At threshold, the integral $J_+(P^0)$ is of order $\mathbf{p}$, while $J_0(P^0)$ is given by

$$J_0(\Sigma_+) = \frac{\mathrm{i}\mu_0^{3/2}}{\sqrt{2}\pi} \sqrt{\Sigma_+ - \Sigma_0}. \tag{D.5}$$

We now include the Coulomb interaction. The self-energy diagram with one virtual Coulomb photon vanishes, because the integration contour over the zero momentum of the photon can be closed in the upper half-plane, where there is no singularity. Next, we evaluate the Coulomb vertex function V_{C} and the two-loop integral B_{C}. The Coulomb vertex function, see for example Fig. 1a, is given by

$$\begin{aligned} V_{\mathrm{C}}(\mathbf{p}, P^0) = -e^2 \frac{1}{\mathrm{i}} \int \frac{\mathrm{d}^D l}{(2\pi)^D} \frac{1}{|\mathbf{p} - \mathbf{l}|^2} \frac{1}{M_{\pi^+} + \frac{\mathbf{l}^2}{2M_{\pi^+}} - l^0} \\ \times \frac{1}{M_{K^+} + \frac{\mathbf{l}^2}{2M_{K^+}} - P^0 + l^0}. \end{aligned} \tag{D.6}$$

After integrating over the zero-component of the loop momentum, the function amounts to

$$V_{\mathrm{C}}(\mathbf{p}, P^0) = e^2 \int \frac{\mathrm{d}^d \mathbf{l}}{(2\pi)^d} \frac{1}{|\mathbf{p} - \mathbf{l}|^2} \frac{1}{P^0 - \Sigma_+ - \frac{\mathbf{l}^2}{2\mu_+}}. \tag{D.7}$$

The contribution to the scattering amplitude is obtained for $P^0 = \omega_{\pi^+}(\mathbf{p}) + \omega_{K^+}(\mathbf{p})$. We expand the function around threshold which leads to

$$V_{\mathrm{C}}(\mathbf{p}, P^0_{\mathrm{thr}}) = -\frac{\pi\alpha\mu_+}{2|\mathbf{p}|} - \mathrm{i}\alpha\theta_{\mathrm{c}} + \mathcal{O}(d-3), \tag{D.8}$$

where $P^0_{\mathrm{thr}} = \Sigma_+ + \frac{\mathbf{p}^2}{2\mu_+}$ and the infrared-divergent Coulomb phase θ_{c} is specified in (3.27). The two-loop Coulomb photon exchange diagram depicted in Fig. 1c reads

$$\begin{aligned} B_{\mathrm{C}}(P^0) = -e^2 \int \frac{\mathrm{d}^D l_1}{(2\pi)^D} \frac{\mathrm{d}^D l_2}{(2\pi)^D} \frac{1}{|\mathbf{l}_1 - \mathbf{l}_2|^2} \\ \times \frac{1}{M_{\pi^+} + \frac{\mathbf{l}_1^2}{2M_{\pi^+}} - l_1^0} \frac{1}{M_{K^+} + \frac{\mathbf{l}_1^2}{2M_{K^+}} - P^0 + l_1^0} \\ \times \frac{1}{M_{\pi^+} + \frac{\mathbf{l}_2^2}{2M_{\pi^+}} - l_2^0} \frac{1}{M_{K^+} + \frac{\mathbf{l}_2^2}{2M_{K^+}} - P^0 + l_2^0}. \end{aligned} \tag{D.9}$$

Performing the integrations over the zero-components of the loop momenta l_1 and l_2, we get

$$\begin{aligned} B_{\mathrm{C}}(P^0) = e^2 \int \frac{\mathrm{d}^d \mathbf{l}_1}{(2\pi)^d} \frac{\mathrm{d}^d \mathbf{l}_2}{(2\pi)^d} \\ \times \frac{1}{|\mathbf{l}_1 - \mathbf{l}_2|} \frac{1}{P^0 - \Sigma_+ - \frac{\mathbf{l}_1^2}{2\mu_+}} \frac{1}{P^0 - \Sigma_+ - \frac{\mathbf{l}_2^2}{2\mu_+}}. \end{aligned} \tag{D.10}$$

The expansion in the vicinity of the threshold amounts to

$$\begin{aligned} B_{\mathrm{C}}(P^0_{\mathrm{thr}}) = -\frac{\alpha\mu_+^2}{2\pi} \left[\Lambda(\mu) + 2\ln\frac{2|\mathbf{p}|}{\mu} - 1 - \mathrm{i}\pi \right] \\ + \mathcal{O}(d-3). \end{aligned} \tag{D.11}$$

The ultraviolet pole term $\Lambda(\mu)$ is given in (C.5).

In the presence of transverse photons, the non-relativistic integrals have to be treated properly in order to avoid loop momenta coming from the hard scale. Otherwise, these loop corrections lead to a breakdown of the non-relativistic counting scheme. We use the threshold expansion [55,56] to disentangle the hard scale (given by the

meson masses) from the soft scales. We illustrate the procedure for the two-point function of the charged pions and kaons at order e^2,

$$\begin{aligned}&\mathrm{i}\int \mathrm{d}x \mathrm{e}^{\mathrm{i}px}\langle 0|Th_\pm(x)h_\pm^\dagger(0)|0\rangle\\&=\frac{1}{M_+ + \frac{\mathbf{p}^2}{2M_+} - p^0 - \Sigma_h(p^0,\mathbf{p})},\end{aligned}\tag{D.12}$$

where $h=\pi, K$ and M_+ denotes the corresponding mass. The self-energy Σ_h is depicted in Fig. 4a (upper line). In $D\neq 4$ space-time dimensions, we have

$$\begin{aligned}&\Sigma_h(p^0,\mathbf{p})\\&=\frac{e^2}{M_+^2}\frac{1}{\mathrm{i}}\int\frac{\mathrm{d}^Dk}{(2\pi)^D}\frac{\mathbf{p}^2-(\mathbf{p}\cdot\mathbf{k})^2/\mathbf{k}^2}{-k^2\left(M_+ + \frac{(\mathbf{p}-\mathbf{k})^2}{2M_+} - p^0 + k^0\right)}\\&\quad+\mathcal{O}(e^4).\end{aligned}\tag{D.13}$$

After integrating over the zero-component of the loop momentum, we arrive at

$$\begin{aligned}&\Sigma_h(p^0,\mathbf{p})\\&=\frac{e^2}{M_+^2}\int\frac{\mathrm{d}^d\mathbf{k}}{(2\pi)^d}\frac{1}{2|\mathbf{k}|}\frac{\mathbf{p}^2-(\mathbf{p}\cdot\mathbf{k})^2/\mathbf{k}^2}{\Omega+\frac{\mathbf{k}^2}{2M_+}-\frac{\mathbf{p}\cdot\mathbf{k}}{M_+}+|\mathbf{k}|}\\&\quad+\mathcal{O}(e^4),\end{aligned}\tag{D.14}$$

where $\Omega = M_+ + \mathbf{p}^2/(2M_+) - p^0$. The threshold expansion amounts to expanding the integrand in (D.14) in the small parameter v, according to the counting[9],

$$\mathbf{k}=\mathcal{O}(v^2),\quad \mathbf{p}=\mathcal{O}(v),\quad \Omega=\mathcal{O}(v^2).\tag{D.15}$$

The threshold expanded self-energy,

$$\hat{\Sigma}_h(\Omega,\mathbf{p})=\frac{e^2}{2M_+^2}\mathbf{p}^2\Omega^{d-2}\frac{\Gamma(d)\Gamma(2-d)}{(4\pi)^{d/2}\Gamma\left(1+\frac{d}{2}\right)}+\mathcal{O}(e^4),\tag{D.16}$$

contains an ultraviolet divergence as $d\to 3$,

$$\begin{aligned}\hat{\Sigma}_h(\Omega,\mathbf{p})&=\frac{e^2}{6\pi^2M_+^2}\mathbf{p}^2\Omega\left(L(\mu)+\ln\frac{2\Omega}{\mu}-\frac{1}{3}\right)\\&\quad+\mathcal{O}(e^4,d-3),\\L(\mu)&=\mu^{d-3}\left[\frac{1}{d-3}-\frac{1}{2}\left(\Gamma'(1)+\ln 4\pi+1\right)\right].\end{aligned}\tag{D.17}$$

E Unitarity condition: Evaluation of the width

The unitarity condition in (5.17) renders the evaluation of the S-wave decay width at next-to-leading order straightforward. It can be seen from (5.18) and (5.19) that in order to evaluate the width at $\mathcal{O}(\delta^{9/2})$, it suffices to calculate the matrix element ${}_+\langle\mathbf{p}|\,\bar{\tau}(E_n)\,|\mathbf{p}_3\rangle_0$ at order δ. Here, the following term occurs

$$\begin{aligned}\Gamma_{n0,\pi^0K^0}&=-C_2^2\frac{M_{\pi^0}^3+M_{K^0}^3}{8M_{\pi^0}^3M_{K^0}^3}|\Psi_{n0}(\mathbf{x}=0)|^2\\&\times\int\mathrm{d}\nu(\mathbf{p}_3)2\pi\delta\left(E_n-\Sigma_0-\frac{\mathbf{p}_3^2}{2\mu_0}\right)\\&\times\mathbf{p}_3^4\left[\frac{1}{z-\Sigma_0-\frac{\mathbf{p}_3^2}{2\mu_0}}+\frac{1}{\bar{z}-\Sigma_0-\frac{\mathbf{p}_3^2}{2\mu_0}}\right]\Bigg|_{z\to E_n+\mathrm{i}\epsilon}+\cdots,\end{aligned}\tag{E.1}$$

which is generated by the matrix element ${}_+\langle\mathbf{p}\,|\,\mathbf{H}_\mathrm{S}\mathbf{G}_\mathrm{C}(z)\mathbf{H}_\mathrm{D}\,|\mathbf{p}_3\rangle_0$ and its hermitian conjugate. This contribution can be calculated by the use of

$$\begin{aligned}&-2\pi\mathrm{i}\delta\left(E_n-\Sigma_0-\frac{\mathbf{p}_3^2}{\mu_0}\right)\\&=\frac{1}{z-\Sigma_0-\frac{\mathbf{p}_3^2}{\mu_0}}-\frac{1}{\bar{z}-\Sigma_0-\frac{\mathbf{p}_3^2}{\mu_0}}\Bigg|_{z\to E_n+\mathrm{i}\epsilon},\end{aligned}\tag{E.2}$$

and the result for the decay width at order $\delta^{9/2}$ agrees with (3.20).

[9] Instead of first performing the integration over the zero-component of the photon field, we may apply the threshold expansion directly to (D.13), with $k^0=\mathcal{O}(v^2)$.

References

1. B. Adeva et al., CERN-SPSLC-95-1, SPIRES entry
2. V. Brekhovskikh, in Proceedings of the Workshop HadAtom03, 13–17 October 2003, ETC* (Trento, Italy), edited by J. Gasser, A. Rusetsky, J. Schacher, p. 9 [hep-ph/0401204]
3. S. Weinberg, Phys. Rev. Lett. **17**, 616 (1966); J. Gasser, H. Leutwyler, Phys. Lett. B **125**, 321 (1983); J. Bijnens, G. Colangelo, G. Ecker, J. Gasser, M.E. Sainio, Phys. Lett. B **374**, 210 (1996) [hep-ph/9511397]; J. Bijnens, G. Colangelo, G. Ecker, J. Gasser, M.E. Sainio, Nucl. Phys. B **508**, 263 (1997) [Erratum B **517**, 639 (1998)] [hep-ph/9707291]; J. Nieves, E. Ruiz Arriola, Eur. Phys. J. A **8**, 377 (2000) [hep-ph/9906437]; G. Amoros, J. Bijnens, P. Talavera, Nucl. Phys. B **585**, 293 (2000) [Erratum B **598**, 665 (2001)] [hep-ph/0003258]
4. G. Colangelo, J. Gasser, H. Leutwyler, Phys. Lett. B **488**, 261 (2000) [hep-ph/0007112]
5. G. Colangelo, J. Gasser, H. Leutwyler, Nucl. Phys. B **603**, 125 (2001) [hep-ph/0103088]
6. L. Rosselet et al., Phys. Rev. D **15**, 574 (1977); C.D. Froggatt, J.L. Petersen, Nucl. Phys. B **129**, 89 (1977); M.M. Nagels et al., Nucl. Phys. B **147**, 189 (1979); A.A. Bolokhov, M.V. Polyakov, S.G. Sherman, Eur. Phys. J. A **1**, 317 (1998) [hep-ph/9707406]; D. Pocanic, hep-ph/9809455; CHAOS Collaboration, J.B. Lange et al., Phys. Rev. Lett. **80**, 1597 (1998); J.B. Lange et al., Phys. Rev. C **61**, 025201 (2000); NA48 Collaboration, R. Batley et al., CERN-SPSC-2000-003, SPIRES entry; S. Pislak et al. [BNL-E865 Collaboration], Phys. Rev. Lett. **87**, 221801 (2001) [hep-ex/0106071]; S. Descotes-Genon, N.H. Fuchs, L. Girlanda, J. Stern, Eur. Phys. J. C **24**, 469

(2002) [hep-ph/0112088]; S. Pislak et al., Phys. Rev. D **67**, 072004 (2003) [hep-ex/0301040]; V.N. Maiorov, O.O. Patarakin, hep-ph/0308162
7. M. Knecht, B. Moussallam, J. Stern, N.H. Fuchs, Nucl. Phys. B **457**, 513 (1995) [hep-ph/9507319]; B **471**, 445 (1996) [hep-ph/9512404]; L. Girlanda, M. Knecht, B. Moussallam, J. Stern, Phys. Lett. B **409**, 461 (1997) [hep-ph/9703448]
8. B. Adeva et al., CERN-SPSC-2000-032, SPIRES entry; L. Afanasyev et al., Lifetime measurement of $\pi^+\pi^-$ and $\pi^\pm K^\mp$ atoms to test low energy QCD (2002), letter of intent of the experiment at Japan Proton Accelerator Research Complex; L. Afanasyev et al., Letter of intent for lifetime measurement of $\pi^+\pi^-$ and $\pi^\pm K^\mp$ atoms to test low energy QCD at the new international research facility at the GSI laboratory; available at http://dirac.web.cern.ch/DIRAC/future.html
9. S. Deser, M.L. Goldberger, K. Baumann, W. Thirring, Phys. Rev. **96**, 774 (1954)
10. T.R. Palfrey, J.L. Uretsky, Phys. Rev. **121**, 1798 (1961)
11. S.M. Bilenky, V.H. Nguyen, L.L. Nemenov, F.G. Tkebuchava, Yad. Fiz. **10**, 812 (1969) [Sov. J. Nucl. Phys. **10**, 469 (1969)]
12. T.L. Trueman, Nucl. Phys. **26**, 57 (1961)
13. U. Moor, G. Rasche, W.S. Woolcock, Nucl. Phys. A **587**, 747 (1995); A. Gashi, G. Rasche, G.C. Oades, W.S. Woolcock, Nucl. Phys. A **628**, 101 (1998) [nucl-th/9704017]; A. Gashi, G.C. Oades, G. Rasche, W.S. Woolcock, Nucl. Phys. A **699**, 732 (2002) [hep-ph/0108116]
14. P. Minkowski, in Proceedings of the International Workshop Hadronic Atoms and Positronium in the Standard Model, Dubna, 26–31 May 1998, edited by M.A. Ivanov et al., Dubna 1998, p. 74 [hep-ph/9808387]
15. G.V. Efimov, M.A. Ivanov, V.E. Lyubovitskij, Sov. J. Nucl. Phys. **44**, 296 (1986) [Yad. Fiz. **44**, 460 (1986)]
16. A.A. Belkov, V.N. Pervushin, F.G. Tkebuchava, Sov. J. Nucl. Phys. **44**, 300 (1986) [Yad. Fiz. **44**, 466 (1986)]
17. M.K. Volkov, Theor. Math. Phys. **71**, 606 (1987) [Teor. Mat. Fiz. **71**, 381 (1987)]
18. Z.K. Silagadze, Sov. Phys. JETP Lett. **60**, 689 (1994) [hep-ph/9411382]; hep-ph/9803307; E.A. Kuraev, Phys. Atom. Nucl. **61**, 239 (1998); U. Jentschura, G. Soff, V. Ivanov, S.G. Karshenboim, Phys. Lett. A **241**, 351 (1998)
19. V.E. Lyubovitskij, A. Rusetsky, Phys. Lett. B **389**, 181 (1996) [hep-ph/9610217]; V.E. Lyubovitskij, E.Z. Lipartia, A.G. Rusetsky, Sov. Phys. JETP Lett. **66**, 783 (1997) [hep-ph/9801215]; M.A. Ivanov, V.E. Lyubovitskij, E.Z. Lipartia, A.G. Rusetsky, Phys. Rev. D **58**, 094024 (1998) [hep-ph/9805356]
20. H. Jallouli, H. Sazdjian, Phys. Rev. D **58**, 014011 (1998) [Erratum D **58**, 099901 (1998)] [hep-ph/9706450]; H. Sazdjian, hep-ph/9809425; Phys. Lett. B **490**, 203 (2000) [hep-ph/0004226]
21. P. Labelle, K. Buckley hep-ph/9804201; X. Kong, F. Ravndal, Phys. Rev. D **59**, 014031 (1999); **61**, 077506 (2000) [hep-ph/9905539]; B.R. Holstein, Phys. Rev. D **60**, 114030 (1999) [nucl-th/9901041]; A. Gall, J. Gasser, V.E. Lyubovitskij, A. Rusetsky, Phys. Lett. B **462**, 335 (1999) [hep-ph/9905309]; D. Eiras, J. Soto, Phys. Rev. D **61**, 114027 (2000) [hep-ph/9905543]; V. Antonelli, A. Gall, J. Gasser, A. Rusetsky, Ann. Phys. (NY) **286**, 108 (2001) [hep-ph/0003118]
22. D. Eiras, J. Soto, Phys. Lett. B **491**, 101 (2000) [hep-ph/0005066]
23. J. Gasser, V.E. Lyubovitskij, A. Rusetsky, A. Gall, Phys. Rev. D **64**, 016008 (2001) [hep-ph/0103157]
24. W.E. Caswell, G.P. Lepage, Phys. Lett. B **167**, 437 (1986)
25. V.E. Lyubovitskij, A. Rusetsky, Phys. Lett. B **494**, 9 (2000) [hep-ph/0009206]
26. J. Gasser, M.A. Ivanov, E. Lipartia, M. Mojzis, A. Rusetsky, Eur. Phys. J. C **26**, 13 (2002) [hep-ph/0206068]
27. P. Zemp, in Proceedings of the Workshop HadAtom03, 13–17 October 2003, ETC* (Trento, Italy), edited by J. Gasser, A. Rusetsky, J. Schacher, p. 18 [hep-ph/0401204]
28. U.G. Meissner, U. Raha, A. Rusetsky, hep-ph/0402261
29. H.W. Hammer, J.N. Ng, Eur. Phys. J. A **6**, 115 (1999) [hep-ph/9902284]
30. J. Gasser, V.E. Lyubovitskij, A. Rusetsky, Phys. Lett. B **471**, 244 (1999) [hep-ph/9910438]
31. J. Schweizer, Phys. Lett. B **587**, 33 (2004) [hep-ph/0401048]. The calculation of the same quantities in the framework of constrained Bethe–Salpeter equation is in progress [32]
32. H. Sazdjian, private communication
33. P. Buettiker, S. Descotes-Genon, B. Moussallam, hep-ph/0310283
34. V. Bernard, N. Kaiser, U.G. Meissner, Phys. Rev. D **43**, 2757 (1991)
35. A. Roessl, Nucl. Phys. B **555**, 507 (1999) [hep-ph/9904230]
36. A. Nehme, Eur. Phys. J. C **23**, 707 (2002) [hep-ph/0111212]; B. Kubis, U.G. Meissner, Phys. Lett. B **529**, 69 (2002) [hep-ph/0112154]
37. J. Bijnens, P. Dhonte, P. Talavera, hep-ph/0404150
38. J. Gasser, H. Leutwyler, Nucl. Phys. B **250**, 465 (1985)
39. S. Descotes-Genon, L. Girlanda, J. Stern, J. High Energy Phys. **0001**, 041 (2000) [hep-ph/9910537]; B. Moussallam, J. High Energy Phys. **0008**, 005 (2000) [hep-ph/0005245]; S. Descotes-Genon, L. Girlanda, J. Stern, Eur. Phys. J. C **27**, 115 (2003) [hep-ph/0207337]; S. Descotes-Genon, N.H. Fuchs, L. Girlanda, J. Stern, hep-ph/0311120
40. A. Nandy, Phys. Rev. D **5**, 1531 (1972)
41. I.T. Todorov, Phys. Rev. D **3**, 2351 (1971)
42. H. Jallouli, H. Sazdjian, Ann. Phys. (NY) **253**, 376 (1997) [hep-ph/9602241]
43. G.J.M. Austen, J.J. de Swart, Phys. Rev. Lett. **50**, 2039 (1983)
44. G.E. Pustovalov, JETP **5**, 1234 (1957); S.G. Karshenboim, Can. J. Phys. **76**, 169 (1998); S.G. Karshenboim, U.D. Jentschura, V.G. Ivanov, G. Soff, Eur. Phys. J. D **2**, 209 (1998)
45. J. Wess, B. Zumino, Phys. Lett. B **37**, 95 (1971)
46. J. Bijnens, L. Girlanda, P. Talavera, Eur. Phys. J. C **23**, 539 (2002) [hep-ph/0110400]
47. H. Feshbach, Ann. Phys. (NY) **5**, 357 (1958); **19**, 287 (1962) [Annals Phys. **281**, 519 (2000)]
48. J. Schwinger, J. Math. Phys. **5**, 1606 (1964)
49. D.R. Yennie, S.C. Frautschi, H. Suura, Ann. Phys. (NY) **13**, 379 (1961)
50. B. Kubis, U.G. Meissner, Nucl. Phys. A **699**, 709 (2002) [hep-ph/0107199]; A. Nehme, P. Talavera, Phys. Rev. D **65**, 054023 (2002) [hep-ph/0107299]
51. B. Kubis, Dissertation Bonn University (2002). Berichte des Forschungszentrums Jülich, 4007 ISSN 0944-2952

52. M. Knecht, R. Urech, Nucl. Phys. B **519**, 329 (1998) [hep-ph/9709348]
53. U.G. Meissner, G. Muller, S. Steininger, Phys. Lett. B **406**, 154 (1997) [Erratum B **407**, 454 (1997)] [hep-ph/9704377]
54. M. Knecht, A. Nehme, Phys. Lett. B **532**, 55 (2002) [hep-ph/0201033]
55. M. Beneke, V.A. Smirnov, Nucl. Phys. B **522**, 321 (1998) [hep-ph/9711391]
56. A.V. Manohar, Phys. Rev. D **56**, 230 (1997) [hep-ph/9701294]; A. Pineda, J. Soto, Nucl. Phys. Proc. Suppl. **64**, 428 (1998) [hep-ph/9707481]; Phys. Lett. B **420**, 391 (1998) [hep-ph/9711292]; Phys. Rev. D **58**, 114011 (1998) [hep-ph/9802365]; **59**, 016005 (1999) [hep-ph/9805424]
57. H. Bethe, E. Salpeter, Quantum mechanics of one- and two-electron atoms (Springer-Verlag, 1957)
58. J. Bijnens, P. Talavera, J. High Energy Phys. **0203**, 046 (2002) [hep-ph/0203049]; S.R. Amendolia et al. [NA7 Collaboration], Nucl. Phys. B **277**, 168 (1986); G. Colangelo, hep-ph/0312017
59. L.L. Nemenov, V.D. Ovsyannikov, E.V. Chaplygin, Nucl. Phys. A **710**, 303 (2002)
60. R. Karplus, A. Klein, Phys. Rev. **87**, 848 (1952)
61. L.L. Nemenov, Sov. J. Nucl. Phys. **41**, 629 (1985) [Yad. Fiz. **41**, 980 (1985)]; L.L. Nemenov, V.D. Ovsyannikov, Phys. Lett. B **514**, 247 (2001)